2009-01-01

Buckling of Dome Structure With Opening, Under Wind Load

Anup Ramesh Marathe
University of Texas at El Paso, armarathe@hotmail.com

BUCKLING OF DOME STRUCTURE WITH OPENING, UNDER WIND LOAD

ANUP RAMESH MARATHE

Department of Civil Engineering

APPROVED:

_____

Cesar Carrasco, Ph.D., Chair

_____

Carlos Ferregut, Ph.D.

_____

John Chessa, Ph.D.

_____

Patricia D. Witherspoon, Ph. D.
Dean of Graduate School

Dedicated

to

My Family

2009

BUCKLING OF DOME STRUCTURE WITH OPENING, UNDER WIND LOAD

by

ANUP RAMESH MARATHE, B.E.

THESIS

Presented to the Faculty of the Graduate School of

The University of Texas at El Paso

in Partial Fulfillment

of the Requirements

for the Degree of

MASTER OF SCIENCE

Department of Civil Engineering

THE UNIVERSITY OF TEXAS AT EL PASO

August 2009

ACKNOWLEDGMENTS

I would like to thank my graduate advisor, Dr. Cesar Carrasco, Associate Professor of Civil Engineering Department at University of Texas at El Paso for giving an opportunity to work for him and also for his continuous support, patience and advice in completing my thesis. It was great experience working with him since I learnt lots of new things.

I would like to thank Dr. Carlos Ferregut for giving me advice whenever needed and giving his valuable time towards attending my thesis defense and assessing my research work. I would also thank Dr. John Chessa for giving his valuable time towards attending my thesis and assessing my research work.

In addition my gratitude goes towards 'GEOMETRICA' for all the information they provided without which this work would have been impossible.

Last but not the least I am grateful to god and my family, specially my father Mr. Ramesh Marathe and my mother Mrs. Rekha Marathe for their continuous support and inspiration. I would like dedicate this work to my grandfather Late Mr. Anant Marathe.

ABSTRACT

Double layered parabolic dome structure, with opening in roof is analyzed for buckling under wind load. Domes with three different opening sizes are used and external wind load is applied from different directions without changing the position of the opening. Dead load and internal wind pressure is also applied. The dead load and internal wind pressure is kept constant. The internal wind pressure is applied as per the ASCE building requirement that is once in positive direction which is towards the surface and once in negative direction which is away from the surface. The data for this project was sent by company 'GEOMETRICA'. A MATLAB program has be developed which is capable of converting this data to a .dat file which is input file for NASTRAN. NASTRAN is a processor which is used for simulations and generates result files. The results can be view using PATRAN which is a pre and post processor. The results obtained in different cases are compared. It can be seen that there is large variation in load carrying capacity of the dome and it can be concluded that the size and the position of the opening has effect on load carrying capacity of the dome.

TABLE OF CONTENTS

LIST OF FIGURES

LIST OF TABLES

1. INTRODUCTION

1.1 Description of problem

A framed structure which has beam-column member is subjected to bending and axial compression under imposed load. When this load exceeds a critical load also known as Euler load, the member will experience out of plane bending and twisting. This kind of situation is called buckling. Euler load is given by $P_{cr} = \Pi^2 / l^2 *(EI)$ where P_{cr} is load acting on member, l is the length of member, E is the Modulus of Elasticity of member, and I is Moment of Inertia. Buckling of member depends on different factors like the length of the member, cross sectional area of member and the support conditions. Buckling can be of various forms like Lateral Buckling, Torsional buckling, Snap through buckling etc. Snap through buckling is a phenomenon where a structure snaps from one stable region to another. Buckling can be catastrophic if it occurs during service period of structure.

Dome structures are widely used these days because of flexibility of geometry which includes long spans without intermediate supports and the ability to resist high wind loads. Dome structures made up of beam-column elements, with openings are subjected to wind load apart from their self weight and live loads. The effect of opening on buckling of dome structures under wind loads is of keen interest. Stress concentrations are more likely to occur near these openings and hence chances of buckling will be more in members near the openings. The geometry of the opening may play an important role in buckling of structure. Hence analysis of domes structures with openings is to be carried out with different opening size under wind load.

Linear and Nonlinear analysis can be performed using different methods. Nonlinear analysis gives accurate results than Linear analysis because the results of Linear analysis are based upon original shape of structures whereas Nonlinear analysis constitutes towards deformed shape of structure. Nonlinear analysis can be carried out using different methods like Newton-Raphson method, Arc-Length method, etc. It is a tedious job to analyze such complicated structures analytically. Numerous finite element software packages are available for performing different types of analysis. NASTRAN will be used here for simulation of Nonlinear analysis and the results can be viewed using PATRAN.

1.2 Objective

The objective of this thesis is to observe the behavior of dome with opening, for buckling, when subjected to wind load from different directions. Dome structures with variations in opening size will be used for analysis. Nonlinear incremental analysis will be performed by applying wind loads from different directions. NASTRAN will be used as a processor for performing analysis which is formatted for different types of analysis which includes Nonlinear analysis. The buckled mode or shape of structure can be viewed in PATRAN which is a pre and post processor. The results obtained will give a better understanding of the behavior of dome structures with openings, for buckling, when subjected to wind load from different direction and ultimately help in improving the designing of members and connections.

1.3 Literature Review

Wu C. C and Arora. J.S. (1988) derived a simple and effective procedure for calculating design of nonlinear critical load which uses load incrimination procedure of non linear analysis which is same as that one used for design sensitivity analysis. In addition it needs mode shape of buckled structure. The sensitivity analysis can be combined with other constraints to optimize structures.

Kato. S, Mutoh. I, and Shomura. M. (1994) studied the effect of semi rigidity at joints on the buckling strength of single layer lattice domes. It was found that buckling loads can be estimated by using strength curves which can be expressed in terms of modified generalized slenderness Λ_{mod} which reflects the reduction β (k) of elastic buckling loads due to semi rigidity parameter k at connections and this curve is proved similar to spherical shells because of non linearity before buckling load and imperfection sensitivity.

Fujito.M, Imai. K, and Saka. T. (1994) conducted experiments on single layer lattice domes under uniform nodal gravity load. Discrete treatment method was used here to calculate buckling behavior. It was proved that buckling load is nearly proportional to half open angle subtended by member and discrete treatment method is applicable for tracing the fundamental equilibrium path and calculating the buckling load.

Ragavan. V, Amde. M.A. (1999) investigated the nonlinear buckling phenomenon of prestressed domes using nonlinear finite element model. A prestressed dome was formed by buckling its individual flat members in arch frame work and stiffened by cable loops in circumferential direction. Incremental load was applied using Newton Raphson iteration with Crisfield's modified arc length to trace non linear path of equilibrium which proved that domes with stiffeners buckle at higher load than unstiffened domes.

Hiyama. Y, Takashima. H, Iijama. T, and Kato. S.(2000) conducted experiments and buckling strength of domes with 3 degree,4 degree and 5 degree of subtended half angle was determined which showed that dome strength with 3 or high degree is determined by individual members with slenderness ranging between 60-80. The observed values and calculated values were compared and correction factor was applied which is used for calculation of slenderness ratio. The analytical and experimental results of material and geometrical non linear analysis were good except for deformation property in elasto plastic region, propagation of yielded members and behavior after buckling.

Ragavan. V, Amde. M. A. (2000) conducted experiments to determine the stability of prestressed domes with external ring stiffeners which resulted in large increase in limit load before collapse and showed significant increase in strength to weight ratio.

Ragavan. V, Amde. M. A. (2002) conducted experiments on prestressed (prebuckled) with flexible or rigid stiffeners and rigid domes which showed that both type of domes reached limit points without bifurcation tendency and reach much higher second peak load. It was proved that stiffeners improve strength to weight ratio of elastic domes and showed improvement in non linear buckling behavior including in post buckling range.

Lopez. A, Puente. I, and Serna. M.A. developed a new beam element with semi rigid joints that allows more exact analysis of load carrying capability and stability of latticed space structures. Theoretical and experimental results were obtained by studying the nonlinear behavior of single layer domes. It has been proved that stiffening the joints avoids negative values in load displacement curve and eliminates the risk of snap through buckling.

2. DESCRIPTION OF BUCKLING THEORY

2.1 Buckling theory

Buckling is a phenomenon, where failure mode is characterized by sudden failure of structural member, subjected to compressive stresses which can be significantly lower than the yield stress. Failure due to buckling mainly depends on elastic modulus and geometric properties of the structural elements. Curvature, load eccentricity and imperfections even if small have a big effect on the buckling capacity of a member. Buckling can be analyzed with different methods like potential energy method, numerical method and few approximate methods are also used which are similar to finite element method.

A simple beam-column element is used to describe the phenomenon of buckling as shown in figure below.

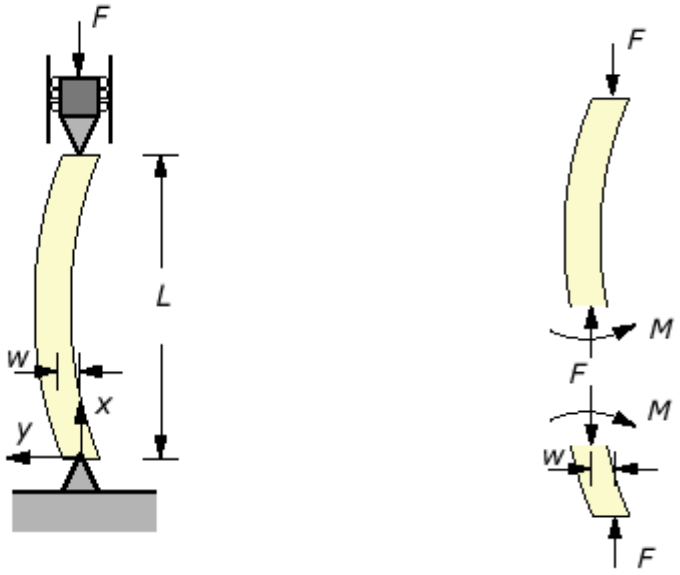

Figure 2.1 (a) Simply Supported Column With Axial Load F (b) Free Body Diagram

Initially the column is assumed to be perfectly elastic and stresses do not exceed the proportional limit. If the load F is less than critical load the column remains straight and undergoes axial compression. When F exceeds the critical load the column becomes unstable and experiences out of plane bending that is the column begins to deflect as shown in Figure 2.1(a). The critical load or the Euler load is maximum axial load on column just before it begins to buckle which is given by $F_{cr} = \prod^2 * EI / L^2$ which can be derived from differential equations, where E is Young's Modulus of column material, I is moment of inertia of cross section and L is effective length of column which depends on boundary conditions and is generally used in column design. Figure 2.1(b) shows the forces and moments acting within the column. A short column fails when the stresses in the column exceed the yield stresses. Material starts yielding when the stresses in it exceed the elastic limit. Buckling can be expected in slender long columns. In intermediate columns buckling occurs after stresses exceed proportionality limit but are less than the ultimate stresses. This is inelastic buckling. Hence short columns are dominated by strength of material, long columns by elastic limit and intermediate columns by inelastic limit of member.

As already mentioned, different methods are available for calculating the buckling capacity of structures. The energy methods used for analysis and calculation of buckling involves tedious calculations and hence are limited to simple or discrete structures. The calculations become much complex as the structure becomes continuous. Approximate methods provide solution to such kind of problems where the continuous structure is replaced by discrete or discontinuous structure. The accuracy of such calculations depends on the number of degrees of freedom. The finite element method and approximate methods are indistinguishable since the objective is similar that is to replace infinite number of degree of freedom structure with that

having finite number of degree of freedom. Rayleigh-Ritz method and Galerkin's method (Background to Buckling; H.G Allen, P.S.Bulson, 1980) are approximate methods generally used. The finite element method is very handy for solving complicated problems with multiple loadings, boundary condition, and complex geometry. Many finite element based software's have been developed which can be used for analysis.

2.2 Theories used in shells and domes.

A shell is basically a thin structure defined as body in which the distance from any point inside the body to some reference surface is small in comparisons with any typical dimensions of the reference surface. The thickness of the shell h as shown in figure below is very small when compared to other dimensions of shell and its radius of curvature. Since the thickness is small bending is neglected and hence the bending moments can be neglected. The shear forces in Q as shown in figure below direction can also be neglected. According to Loves assumptions 1) normal's to the reference surface remains straight and normal during the deformation, and 2) the transverse normal stress is negligibly small. Later these assumptions were modified to remove some inconsistencies. Donnell presented simple set of equations for cylindrical shells and later it was extended for general shallow shells which are referred as Donnell-Mushtari-Vlasov equations(Buckling of Bars, Plates, and Shells. Brush, Almroth. 1975).

The nonlinear equilibrium equations for cylindrical shells can be derived using different methods like, summation of forces and moments, the energy method and there are numerous approximate methods and among them most used is von Karman-Tsien.

Consider a circular cylindrical shell and an element of the cylindrical shell in deformed condition with forces and moments acting on it as shown in the figure.

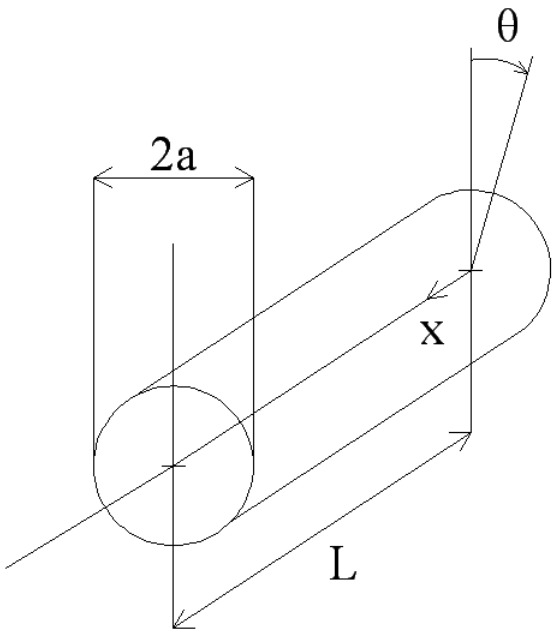

Figure 2.2 Circular Cylindrical Shell

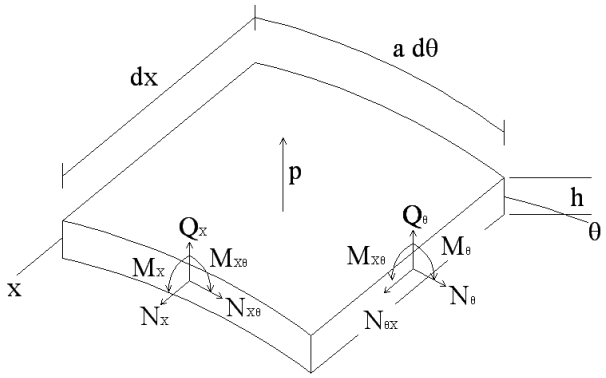

Figure 2.3 Cylindrical Shell Element

Non linear equilibrium equation (Buckling of Bars, Plates, and Shells. Brush, Almroth. 1975). for the above cylindrical shell can be derived by summation of forces and moments as shown in the above figure. The force and moment intensities are related to internal stresses given by following equations.

$$N_x = \int_{-h/2}^{h/2} \bar{\sigma}_x \left(1+\frac{z}{a}\right) dz \ , \qquad N_\theta = \int_{-h/2}^{h/2} \bar{\sigma}_\theta dz \ ,$$

$$N_{x\theta} = \int_{-h/2}^{h/2} \bar{\tau}_{x\theta} \left(1+\frac{z}{a}\right) dz \ , \qquad N_{\theta x} = \int_{-h/2}^{h/2} \bar{\tau}_{\theta x} dz \qquad (2.1)$$

$$Q_x = \int_{-h/2}^{h/2} \bar{\tau}_{xz} \left(1+\frac{z}{a}\right) dz \qquad Q_\theta = \int_{-h/2}^{h/2} \bar{\tau}_{\theta x} dz$$

$$M_x = a\int_{-h/2}^{h/2} \bar{\sigma}_x \left(1+\frac{z}{a}\right) z dz \qquad M_\theta = a\int_{-h/2}^{h/2} \bar{\tau}_{\theta x} z dz$$

$$M_{x\theta} = a\int_{-h/2}^{h/2} \bar{\tau}_{x\theta} \left(1+\frac{z}{a}\right) z dz \qquad M_{\theta x} = a\int_{-h/2}^{h/2} \bar{\tau}_{\theta x} z dz$$

where

a = radius of the cylinder

D = bending stiffness parameter

w = displacement component

N_x , N_θ, $N_{x\theta}$, $N_{\theta x}$ is normal and shear force intensity.

Q_x, Q_θ are transverse shearing force intensities.

M_x, M_θ are bending moment intensities.

$M_{x\theta}$, $M_{\theta x}$ are twisting moment intensities.

Summation of forces gives following equations

$$aN_{x,x} + N_{x\theta,\theta} = 0 \qquad (2.2)$$

$$aN_{x\theta,x} + N_{\theta,\theta} + Q_{\theta} = 0 \qquad (2.3)$$

$$Q_{\theta\theta} + aQ_{x,x} - N_{\theta} - aN_{x}\beta_{x,x} - aN_{x\theta}\beta_{\theta,x} - N_{\theta x}\beta_{x,\theta} - N_{\theta}\beta_{\theta,\theta} = -pa \qquad (2.4)$$

Q is transverse shearing force which can be eliminated by taking moments relative to x and θ directions and by substituting equations 2.5 and 2.6 in above equations.

$$aQ_{\theta} = M_{\theta,\theta} + aM_{x\theta,x} \qquad (2.5)$$

$$aQ_{x} = aM_{x,x} + aM_{\theta x,\theta} \qquad (2.6)$$

For relatively thin cells $N_{\theta x} = N_{x\theta}$ and $M_{\theta x} = M_{x\theta}$

The equilibrium equations obtained are as follows:

$$aN_{x,x} + N_{x\theta,\theta} = 0$$

$$aN_{x\theta,x} + N_{\theta,\theta} = 0 \qquad (2.7)$$

$$a^2 M_{x,xx} + 2aM_{x\theta,x\theta} + M_{\theta,\theta\theta} - aN_{\theta} - a^2 N_{x}\beta_{x,x} - aN_{x\theta}(a\beta_{\theta,x} + \beta_{x,\theta}) - aN_{\theta}\beta_{\theta,\theta} = -pa^2 \qquad (2.8)$$

Consecutive equations for thin walled isotropic cylinders are given as follows:

$$N_{x} = C(\varepsilon_{x} + \nu\varepsilon_{\theta}) \qquad M_{x} = D(k_{x} + \nu k_{\theta})$$

$$N_{\theta} = C(\varepsilon_{\theta} + \nu\varepsilon_{x}) \qquad M_{\theta} = D(k_{\theta} + \nu k_{x}) \qquad (2.9)$$

$$N_{x} = C\frac{1-\nu}{2}\gamma_{x\theta} \qquad M_{x\theta} = D(1-\nu)k_{x\theta}$$

Kinematic relations on which Donnells equations are based are as follows:

$$\varepsilon_{x} = u,_{x} + \frac{1}{2}\beta_{x}^{2} \qquad \beta_{x} = -w,_{x} \qquad k_{x} = \beta_{x,x}$$

$$\varepsilon_\theta = \frac{v_{,\theta} + w}{a} + \frac{1}{2}\beta_x^{\,2} \qquad \beta_\theta = -\frac{w_{,\theta}}{a} \qquad k_\theta = \frac{\beta_{\theta,\theta}}{a} \qquad (2.10)$$

$$\gamma_{x\theta} = \left(\frac{u_{,\theta}}{a} + v_{,x}\right) + \beta_x\beta_\theta \qquad k_{x\theta} = \frac{1}{2}\left(\frac{\beta_{x,\theta}}{a} + \beta_{\theta,x}\right)$$

Substituting constitutive equations and kinematic relations in the equilibrium equations give

$$aN_{x,x} + N_{x\theta,\theta} = 0$$

$$aN_{x\theta,x} + N_{\theta,\theta} = 0$$

$$D\nabla^4 w + \frac{1}{a}N_\theta - \left(N_x w_{,xx} + \frac{2}{a}N_{x\theta}w_{,x\theta} + \frac{1}{a^2}N_\theta w_{,\theta\theta}\right) = p \text{ where} \qquad (2.11)$$

$$\nabla^4 w \equiv w_{,xxxx} + \frac{2}{a^2}w_{,xx\theta\theta} + \frac{1}{a^4}w_{,\theta\theta\theta\theta}$$

Equations 2.11 are nonlinear equilibrium equations for shallow cylindrical shells. These equations have been widely used for large deflection analysis of cylindrical shells.

3. NUMERICAL BUCKLING ANALYSIS

3.1 Introduction

Numerical analysis such as the finite element analysis is handy when the structure is complicated and has multiple loading, boundary conditions and complex geometry. The buckling concept as mentioned earlier for the beam column element can be further extended to building frames, truss, etc. Framed structures are subdivided in two types (a) Elastic rigid jointed frames without sway (b) Rigid jointed frames with sway. The buckling analysis of frame structure is not exactly same as that of a single column. In a framed structure, the buckling capacity of an individual member is a function of the rigidity of the connections and the load (axial and bending moments) on each one of the elements it is connected to. The effect of the load on adjacent elements on the buckling capacity of an individual member is due to the non-linearity of the relationship between element loads and external loads which in not known. This unknown load can be determined by linearizing the second order theory. Initially first order theory is used to calculate the forces in all members based on undeformed shape of the structure. These forces are then treated as known in second order analysis.

3.2 Linear Buckling

A structure is said to be in stable condition when it returns back to its original position once the load is removed. There are certain conditions where the structure may become unstable because of some loading cases. Under such loading cases the structure continues to deflect

without increase in the magnitude the load. Such unstable condition is called buckling. When the structure does not yield and the direction of the forces do not change such condition is considered as linear buckling and the structure is said to be elastically stable. The deflections observed in linear buckling are assumed to be small and the stresses in the elements are assumed to be elastic.

NASTRAN is a finite element based software and hence uses finite element method to solve the linear buckling problem and makes some assumptions other than mentioned previously. Linear buckling problem is addressed by including the effect of differential stiffness matrix to the linear stiffness matrix. The differential stiffness matrix is a function of geometry element type and applied load. Consider a single planar CBAR element with y and θ_z degrees of freedom at each end for simplicity.

Figure 3.1 Single Planar Bar Element

The differential stiffness matrix for such case is given as

$$[k_d]_i = \begin{bmatrix} \frac{6F_{x_i}}{5l_i} & \frac{-F_{x_i}}{10} & \frac{6F_{x_i}}{5l_i} & \frac{-F_{x_i}}{10} \\ \frac{-F_{x_i}}{10} & \frac{2l_iF_{x_i}}{15} & \frac{F_{x_i}}{10} & \frac{-l_iF_{x_i}}{30} \\ \frac{-6F_{x_i}}{5l_i} & \frac{F_{x_i}}{10} & \frac{6F_{x_i}}{5l_i} & \frac{F_{x_i}}{10} \\ \frac{F_{x_i}}{10} & \frac{-lF_{x_i}}{30} & \frac{F_{x_i}}{10} & \frac{2l_iF_{x_i}}{15} \end{bmatrix}$$

Here F_{x_i} is equal to force P_a since there is only one force in X direction and is linear to the member and i is the i-th element. The differential stiffness matrix can also be written as

$$[k_d]_i = P_a \begin{bmatrix} \frac{6\alpha_i}{5l_i} & -\frac{\alpha_i}{10} & \frac{-6\alpha_i}{5l_i} & \frac{-\alpha_i}{10} \\ \frac{-\alpha_i}{10} & \frac{2l_i\alpha_i}{15} & \frac{\alpha_i}{10} & \frac{-l_i\alpha_i}{30} \\ \frac{-6\alpha_i}{5l_i} & \frac{\alpha_i}{10} & \frac{6\alpha_i}{5l_i} & \frac{\alpha_i}{10} \\ \frac{-\alpha_i}{10} & \frac{-l_i\alpha_i}{30} & \frac{\alpha_i}{10} & \frac{2l_i\alpha_i}{15} \end{bmatrix} = P_a \left[\bar{k}_d \right]_i$$

where α_i is the distribution factor of the applied loads to the i-th element. α is different for each member in the structure and depends on element type and orientation of member related to structure, and applied load. The overall stiffness matrix for the system can be represented as

$$[K] = [K_a] + [K_d]$$

where $[K_a]$ and $[K_d]$ are summation of linear and differential matrix.

The total potential matrix is given as

$$[U] = 0.5\{u\}^T [K_a]\{u\} + 0.5\{u\}^T [K_d]\{u\}$$

The above equation will be in equilibrium if it has a stationary value, hence

$$\frac{\partial [U]}{\partial u_i} = [K_a]\{u\} + [K_d]\{u\} = \{0\}$$

Where u_i is the displacement of the i-th term. The above equation can also be written as

$$\left[[K_a] + P_a \left[\bar{K}_d \right] \right] \{u\} = \{0\}$$ where

$[K_d] = P_a \left[\bar{K}_d \right]$ and P_a is applied load

For non trivial solution $\left| [K_a] + P_a \left[\bar{K}_d \right] \right| = \{0\}$

The critical load values are obtained when the above determinant is satisfied.

The number of buckling loads obtained is equal to number of degrees of freedom. That is

$$P_{cr_i} = \lambda_i P_a \qquad (3.4)$$

Equation 3.1 can be written as $\left| [K_a] + \lambda_i [K_d] \right| = [0]$

Equation 3.2 is an Eigen value problem. Once the Eigen values of λ are obtained, critical loads can be obtained from the equation.

3.3 Finite element analysis for buckling of frames

The analysis of buckling of frame structures begins with determination of stiffness or flexibility matrices of members. The stiffness coefficients of structural element represent the force produced by unit displacement. Consider a beam column element as shown in figure below which is perfectly straight elastic beam with length *l* fixed at b and is loaded axially by force P.

Figure 3.2 Fixed – Hinged Beam Subjected to Axial Load P

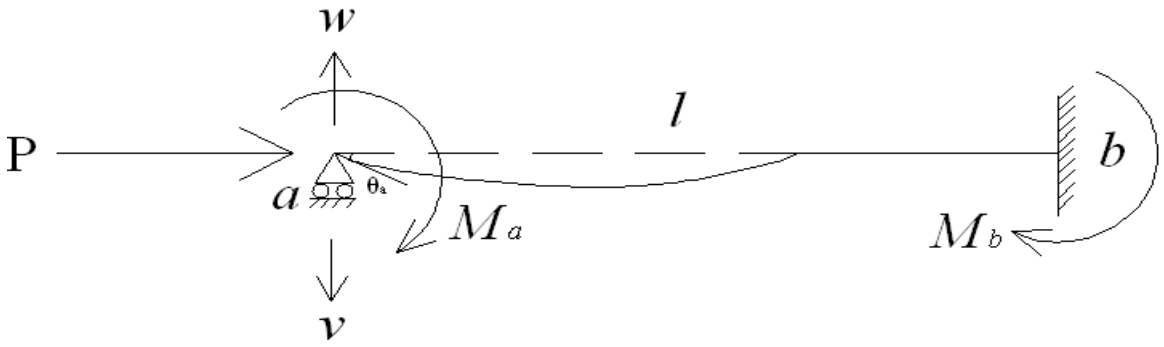

Figure 3.3 Fixed – Hinged Beam Subjected to Axial Load P and End Rotation

The deflection curve of the beam is given by following equation

$$w(x) = A\sin kx + B\cos kx + Cx + D + w_p(x) \qquad (3.1)$$

$w_p(x)$ is displacement due to transverse load which is zero since there is no transverse distributed load.

The boundary conditions are $w=0$ and $w'=-\theta_a$ at x=0 and $w=0$ and $w'=0$ at $x=l$ which leads to

$$\begin{aligned} &B + D = 0 \\ &Ak + C = -\theta_a \\ &A\sin kl + B\cos kl + Cl + D = 0 \\ &Ak\cos kl - Bk\sin kl + C = 0 \end{aligned} \tag{3.2}$$

$$\lambda = kl = \sqrt{\frac{P}{EI}}l \tag{3.3}$$

By eliminating C and D from equation 3.1 we obtain.

$$\begin{aligned} &A(\sin\lambda - \lambda) + B(\cos\lambda - 1) = \theta_a l \\ &A(\cos\lambda - 1) - B\lambda\sin\lambda = \theta_a l \end{aligned} \tag{3.4}$$

By subtracting the above equations we get

$$A = B\left(\frac{1-\cos\lambda - \lambda\sin\lambda}{\sin\lambda - \lambda\cos\lambda}\right) \tag{3.5}$$

B can be obtained by substituting above equation in equation 3.4

Moment about can be given by

$$M_a = K\theta_a \text{ and } M_b = Kc\theta_a \tag{3.6}$$

where $K = sEI/L$ and c is carryover factor.

M_a and M_b given above are for bending moments caused by rotating end a while end b is fixed.

Now keeping end a fixed and rotating end b we obtain

$$M_a = Kc\theta_b \text{ and } M_b = K\theta_b \tag{3.7}$$

The matrix obtained by superposing equations 3.6 and 3.7 is

$$\begin{Bmatrix} M_a \\ M_b \end{Bmatrix} = \frac{EI}{l} \begin{bmatrix} s & sc \\ sc & s \end{bmatrix} \begin{Bmatrix} \theta_a \\ \theta_b \end{Bmatrix} \qquad (3.8)$$

The square matrix in the above equation with EI/*l* is called stiffness matrix.

$$s = \frac{\lambda(\sin\lambda - \lambda\cos\lambda)}{(2 - 2\cos\lambda - \lambda\sin\lambda)} \qquad (3.9.a) \qquad c = \frac{(\lambda - \sin\lambda)}{(\sin\lambda - \lambda\cos\lambda)} \qquad (3.9.b)$$

The inverse of the stiffness matrix gives the flexibility as shown below

$$\begin{Bmatrix} \theta_a \\ \theta_b \end{Bmatrix} = \frac{l}{EI} \begin{bmatrix} \psi_s & -\phi_s \\ -\phi_s & \psi_s \end{bmatrix} \begin{Bmatrix} M_a \\ M_b \end{Bmatrix} \qquad (3.10)$$

The square matrix along with *l* / (EI) in equation *3*.2 is called flexibility matrix.

$$\psi_s = \frac{1}{\lambda}\left(\frac{1}{\lambda} - \cot\lambda\right) \qquad (3.11.a)$$

$$\phi_s = \frac{1}{\lambda}\left(\frac{1}{\sin} - \frac{1}{\lambda}\right) \qquad (3.11.b)$$

and θ_a and θ_b are small rotations imposed at a and b respectively.

Equations 3.9.a, 3.9.b, 3.11.a, 3.11.b are limited to axial compression but when the member is subjected to tension all the parameters that are *s, c, Ψ*$_s$*, Φ*$_s$ become hyperbolic as shown below. These parameter are known as stability functions.

$$s = \frac{\lambda(\lambda\cosh\lambda - \sinh\lambda)}{2 - 2\cosh\lambda + \lambda\sinh\lambda} \qquad c = \frac{\sinh\lambda - \lambda}{\lambda\cosh\lambda - \sinh\lambda} \qquad (3.12)$$

$$\psi_s = \frac{1}{\lambda}\left(\frac{1}{\tanh\lambda} - \frac{1}{\lambda}\right) \qquad \phi_s = \frac{1}{\lambda}\left(\frac{1}{\lambda} - \frac{1}{\sinh\lambda}\right) \qquad (3.13)$$

If there are no axial loads the values of *s* and *c* are 4 and ½ respectively.

Stability functions for beam-columns with shear deformations are given by

$$s = \frac{\lambda \sin\lambda - \lambda^2 \beta \cos\lambda}{2 - 2\cos\lambda - \lambda\beta \sin\lambda} \qquad c = \frac{\lambda\beta - \sin\lambda}{\sin\lambda - \lambda\beta\cos\lambda} \qquad \beta = 1 - \frac{P}{GA_0} \qquad (3.14)$$

It is not always that the frame is rigidly jointed and hence chances of sway should also be taken into consideration.

Consider a beam-column element as shown in figure.

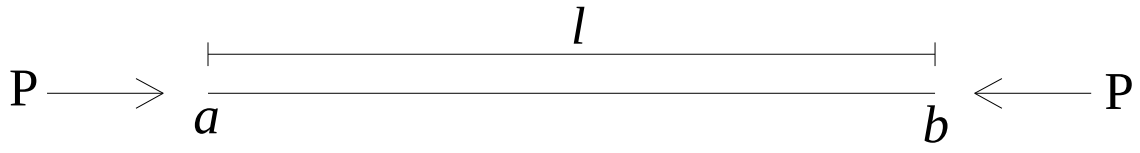

Figure 3.4 Member of a Frame Subjected to Axial Force P

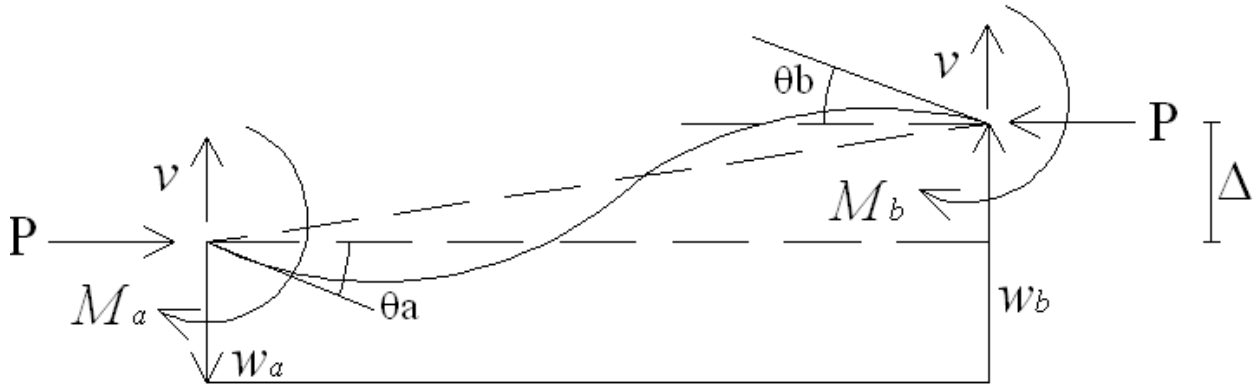

Figure 3.5 End Displacement and Internal Forces in Beam

The beam is subjected to force P which has length l . Small lateral displacement w_a and w_b along with small rotations are θ_a and θ_b are imposed at the ends of the beam. Δ is relative lateral displacement of beam ends.

The stiffness matrix for beam-column element shown above is,

$$\begin{Bmatrix} M_a \\ M_b \\ V \end{Bmatrix} = \frac{EI}{l} \begin{bmatrix} s & sc & \frac{s_1}{l} \\ sc & s & \frac{s_1}{l} \\ \frac{s_1}{l} & \frac{s_1}{l} & \frac{s^*}{l^2} \end{bmatrix} \begin{Bmatrix} \theta_a \\ \theta_b \\ \Delta \end{Bmatrix} + \begin{Bmatrix} M_a^L \\ M_b^L \\ V^L \end{Bmatrix} \qquad (3.15)$$

where $s_1 = s(1+c)$

$$s^* = 2s_1 - \frac{PL^2}{EI} \qquad \text{and}$$

M_a^L, M_b^L , is fixed end moments and

V^L is fixed end shear forces which are produced because of the lateral load.

The values of these can be calculated from the general solution by imposing the boundary conditions. θ_a, θ_b, Δ is incremental displacement starting from initial state of equilibrium under axial force P. Critical load value can be derived by finding the determinant of stiffness matrix and knowing the approximate roots. The accurate value can then be obtained by iterative methods.

Frames with multiple members give rise to more number of unknowns which create computational problems. Consider a frame shown below which is braced against lateral sway and the curvature of the columns is smallest that is the effective length is largest. There is no displacement in the joints and there is only single unknown rotation θ.

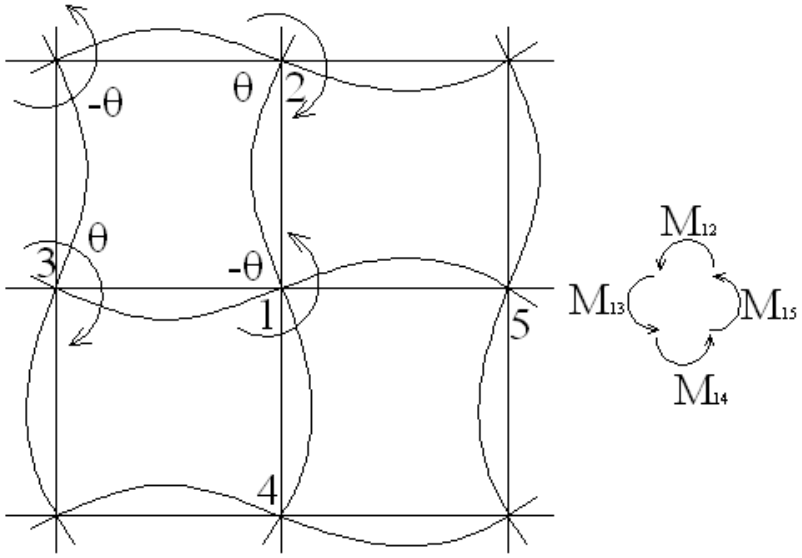

Figure 3.6 Non Sway Buckling of Braced Regular Frame

Hence one equilibrium equation is required which can be obtained by all four moments acting at one joint given by $M_{12} + M_{13} + M_{14} + M_{15} = 0$. Expressing these moments in terms of $M = K\theta$ and $s_{12} = s_{14}$ and $s_{13} = s_{15}$ and since there is no axial force acting on horizontal members we can assume $s_{13} = 4$ and $c_{13} = 0.5$ we have

$$m_{12}\theta + m_{13}\theta = 0$$

$$m_{12} = \frac{2EI_{12}}{l_{12}}\left(s_{12} - s_{12}c_{12}\right) \qquad (3.16)$$

$$m_{13} = \frac{2EI_{13}}{l_{13}}\left(s_{13} - s_{13}c_{13}\right)$$

Assuming bending rigidity and length of members is same equation 3.16 is reduced to

$$D(P) = s_{12}(1 - c_{12}) + 2 = 0. \qquad (3.17)$$

where D(P) is determinant of equation 3.16

Using Newton iterative methods we get the solution for the critical load which is 1.6681 $P_{E.}$

When there is lateral displacement and rotation and assuming the lateral displacement between the floors is same we obtain two equations of equilibrium. Since the lateral deformations are assumed to be same the horizontal shear force applied from the column floors is same and hence the sum must be zero since there is no lateral load applied.

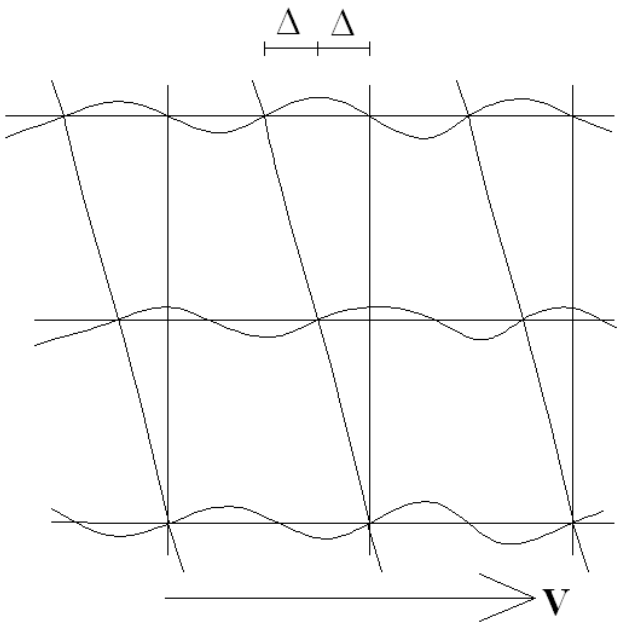

Figure 3.7 Sway Buckling of Members

The two equilibrium conditions obtained are

$$\Sigma M = m_{12}\theta + m_{13}\theta + m_{12}^{s}\Delta = 0 \qquad (3.17)$$

$$\Sigma V = k_{12}\theta + k_{12}^{s}\Delta = 0 \quad \text{where} \qquad (3.18)$$

$$m_{12} = \left(\frac{2EI_{12}}{l_{12}}\right)\left(s_{12} + s_{12}c_{12}\right)$$

$$m_{12}^{s} = -\left(\frac{2EI_{12}}{l_{12}^{2}}\right)$$

$$k_{12} = -\left(\frac{2EI_{12}}{l_{12}^{2}}\right)\bar{s}_{12}$$

$$k_{12}^{s} = \left(\frac{EI}{l_{3}^{12}}\right)s_{12}^{*}$$

$$\bar{s} = s(1+c) \text{ and } s^{*} = 2\bar{s} - \frac{(PL^{2})}{(EI)}$$

Since there are no axial forces in the horizontal members we can substitute $s_{13} = 4$ and $c_{12} = 0.5$ and for non zero deformation to exist the determinant of equation 3.17 and 3.18 must be zero.

Hence we get the equation $D(P) = 2\bar{s}^{2}_{12} - s^{*}_{12}(6 + s_{12}(1+ c_{12}) = 0$.

The critical load for such structure is $0.577\ P_E$.

3.4 Non linear analysis

Nonlinearity is of two types which is (a) Geometric nonlinearity (b) Material nonlinearity. Geometric nonlinearity comes from the non-linear relation between the deformation of the structure and the load. When the nodal displacements of the structure are significant, the load in the individual elements is not only a function of the external loads but also of the deformation. Material non-linearity results from the non-linear material behavior of the materials used to build the structure. In most metals used for structural applications, the material stress-strain relation is characterized by a linear elastic portion under small strains and a nonlinear relation after the stress exceeds the yield point. In a numerical FEM non-linear analysis, the load is added in small increments. After each step, the stiffness of the structure is updated to take into account the effect of the deformed structure and the possibility of stresses exceeding the yield stress.

4.0 MODELLING AND SIMULATIONS

4.1 Structure description and modeling

The dome structure used for analysis is a double layer parabolic frame structure with posts. The diameter of the dome is about 105.8 meters and the height of the dome is about 31.5 meters. The structure is made of steel having modulus of elasticity, E, 199948 MPa and Yield strength and Ultimate strength 290 MPa and 400 MPa respectively. The members used for the dome are of different cross section. Other properties of the bars are given in table below.

Table 4.1 Bar Properties

ID	Bar	D	t	A	I	S	r	J
		mm	mm	mm^2	mm^4	mm^3	mm	mm^4
1	7/8"x 0.090"	47.625	2.286	325.6	83879	3522	16.05	167759
2	3/8"x 0.090"	60.325	2.286	416.8	175780	5828	20.54	351560
3	7/8"x 0.104"	73.025	2.6416	584.1	362200	9920	24.90	724401

The supports of the dome are fixed. Domes with three different opening cases are used. The shape of the opening in all the case is rectangular and the sizes of opening are 9.72m x 4.74m (Figure 4.1) and 16.45m x 10.74m (Figure 4.2) and the third dome is reinforced near opening and has opening size 9.72m x 4.74m (Figure 4.3). The purpose of these domes is for bulk storage of materials and the conveyor belt which transfers the material rests on the opening.

There are also walkways provided on the floor form different directions as shown in the figures below.

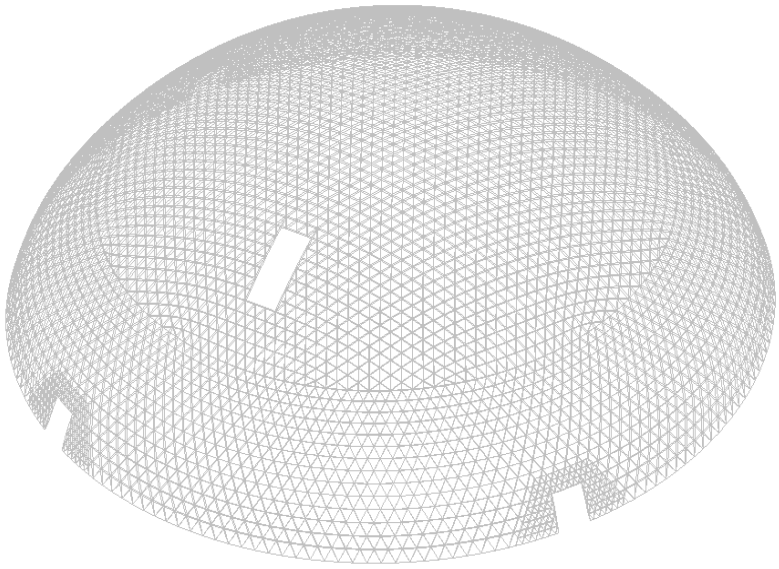

Figure 4.1 Dome with opening size 9.72 m x 4.74 m

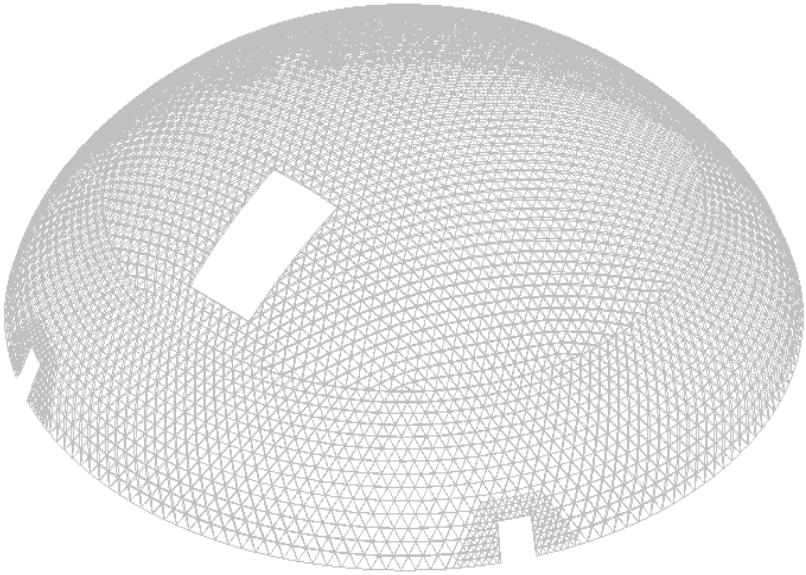

Figure 4.2 Dome with opening size 16. 45 m x 10.74 m

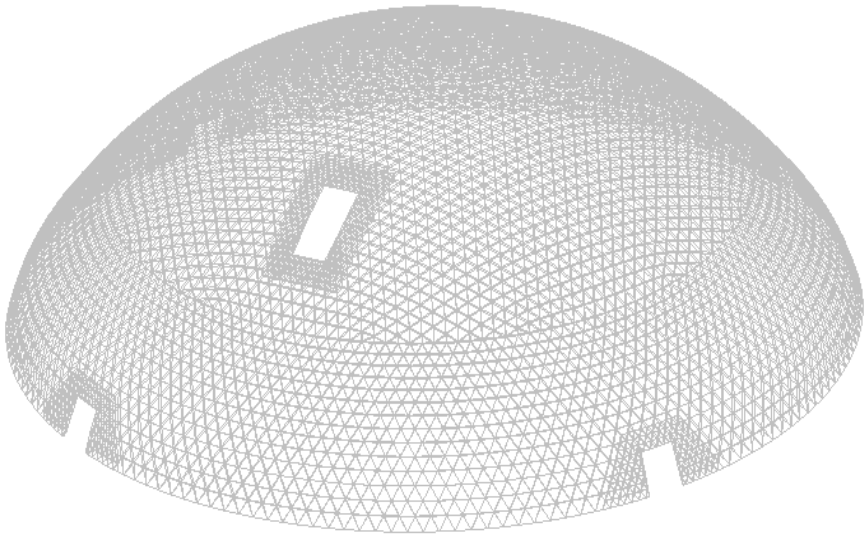

Figure 4.3 Dome with opening size 9.72 m x 4.74 m with reinforcement

The data for these models was sent by company ‘GEOMETRICA’. This data includes the properties of the bar, the position of the nodes with respect to the Cartesian system and the loads. The properties of the bar are specified in table 4.1. The loads consist of dead load, live load, internal wind pressure, and external wind load. These loads were developed from ASCE equations’. A MATLAB program was generated which could read the excel data format sent by the company and convert it to a data file which is read by PATRAN to generate the model. PATRAN is a pre and post processor as mentioned earlier which is used for viewing the dome structure and its results. The ‘.dat’ file generated by MATLAB is also read by NASTRAN which is a processor. When the data is processed various output files with results are generated.

4.2 Simulation Cases

Nonlinear analysis has been performed on the dome structures which use incremental loads as mentioned previously. Different types of loads are acting on the dome structure. The self weight acts in the downward direction that is negative Z axis. As per the ASCE building code requirements the internal pressure should be applied once in positive direction that is towards the roof/surface and once in negative direction which is away from the roof/surface. Analysis for wind load should be dynamic analysis but in this case the wind load is converted to equivalent static load and hence is acting on the dome in horizontal and perpendicular direction. The wind load is applied on structure acting in X, Y, and Z directions as of Cartesian system. There are totally forty eight simulations. For simulation purposes, three (3) different dome opening sizes/reinforcement were considered, two (2) cases of internal pressure direction (one positive and one negative) and eight (8) cases of external wind load pressure corresponding to eight (8) different directions of wind load. Dome with large opening, small opening and one with reinforcement are analyzed for external wind load once with positive internal wind pressure and once with negative internal pressure. In all the cases the dead load and the internal wind pressure is same. The only difference in these cases is the external wind load is applied at an angle incrementing by 45 degrees. Following flow chart (Figure 4.4) shows an example of simulation for dome with three different opening sizes.

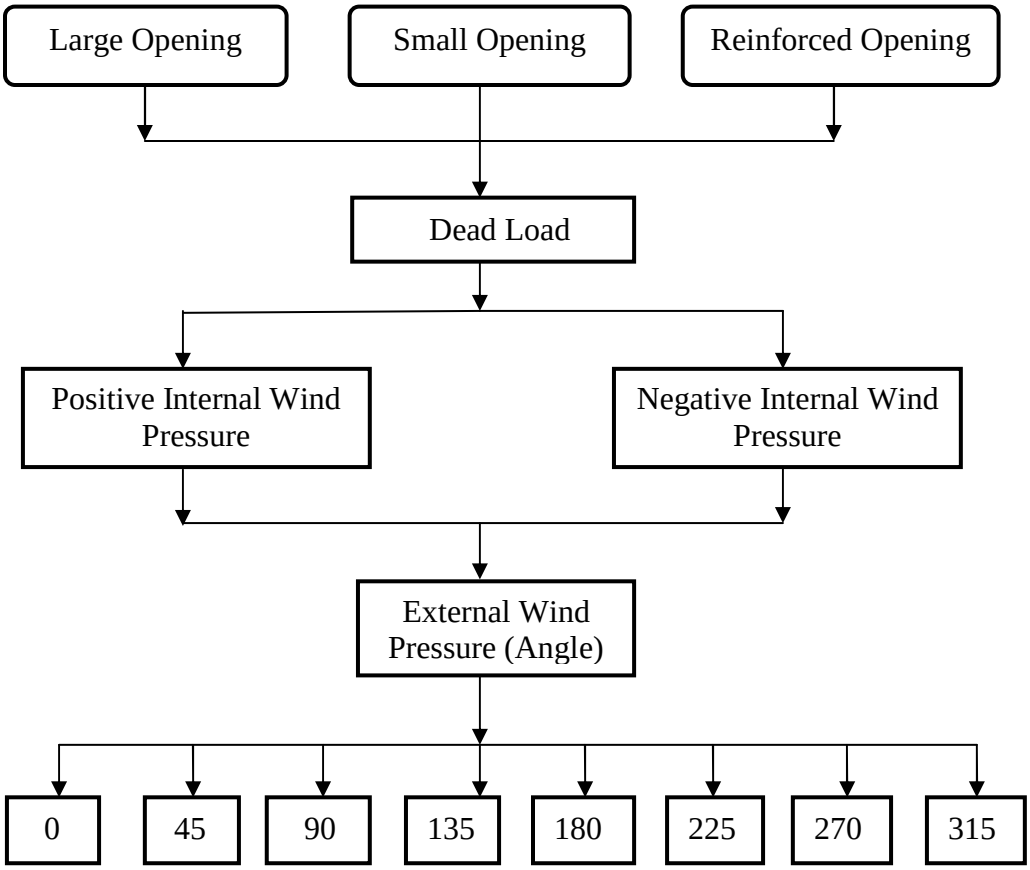

Figure 4.4: Flow chart showing load case for large opening.

As mentioned previously a MATLAB program has been written which generates a dat file. This dat file is an input file that can be read by NASTRAN which is used for running the simulations. It was also mentioned that Nonlinear analysis has been used for simulations and hence load has to be increased until the structure fails. Load can be increased or decreased by changing the factors that has been specified in the MATLAB program (see Appendix) along with number of increments. Dead load initially is applied with factor 1.0 starting with 20% of actual dead load.

Wind load is applied with factor 30. The factor used for wind load is not same for all the simulation cases and varies depending on the dome failure that is the factor is increased till the dome fails. The dead load starts with 20% of its initial value since 5 increments have been specified, that is, it divides the dead load into 5 equal increments. In case of wind load 30 increments have been specified and hence it divides the wind load into 30 equal increments. The maximum percentage load at which the dome fails is used for calculating the final results which is explained in the next chapter. Figure (4.5) show the wind profile (contour) when external wind load acts form 0 degrees and figure 4.6 shows wind profile(contour) when both external and internal wind pressure act together.

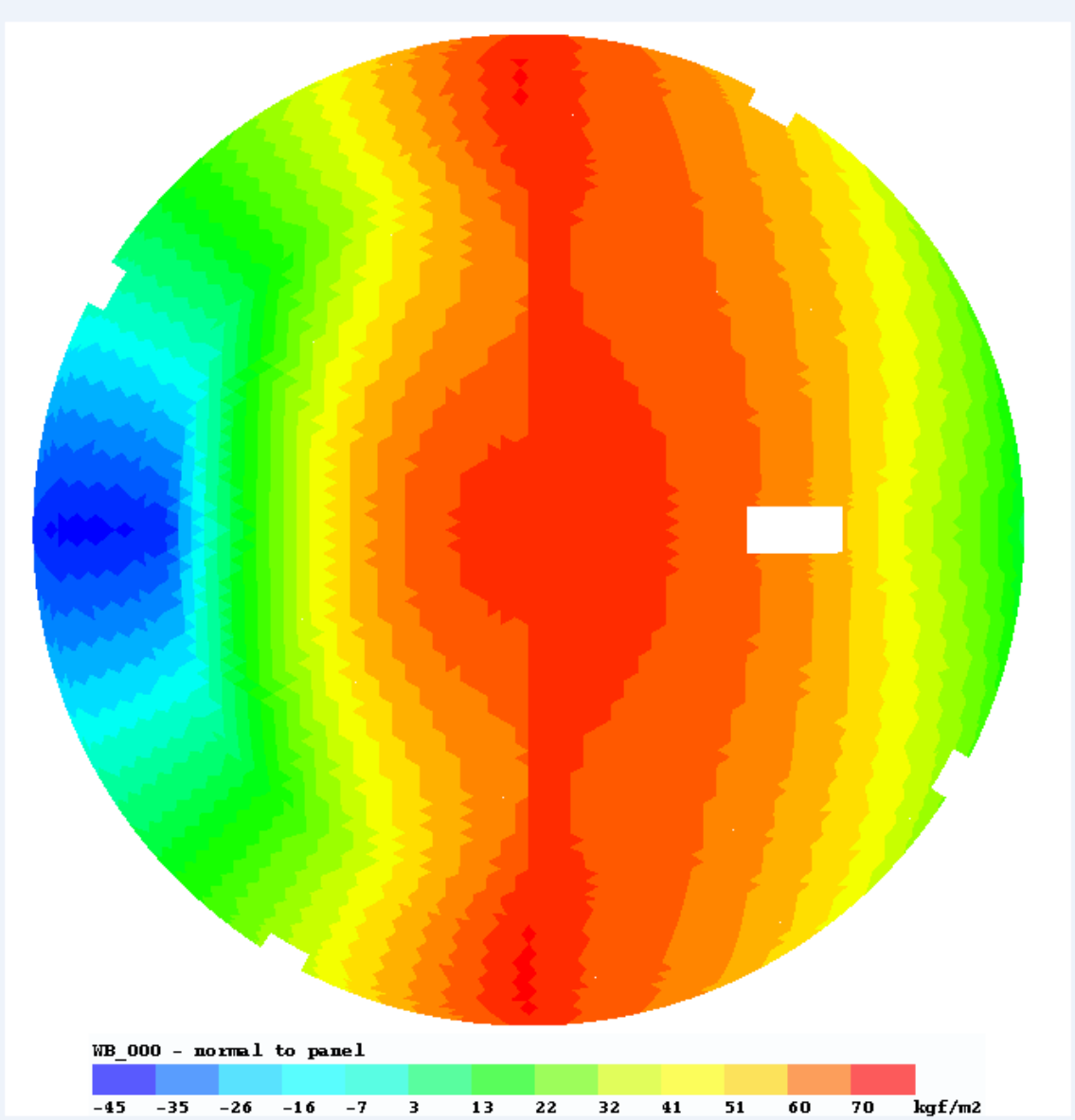

Figure 4.5 Contour for dome with small opening, wind load acting at 0 degrees

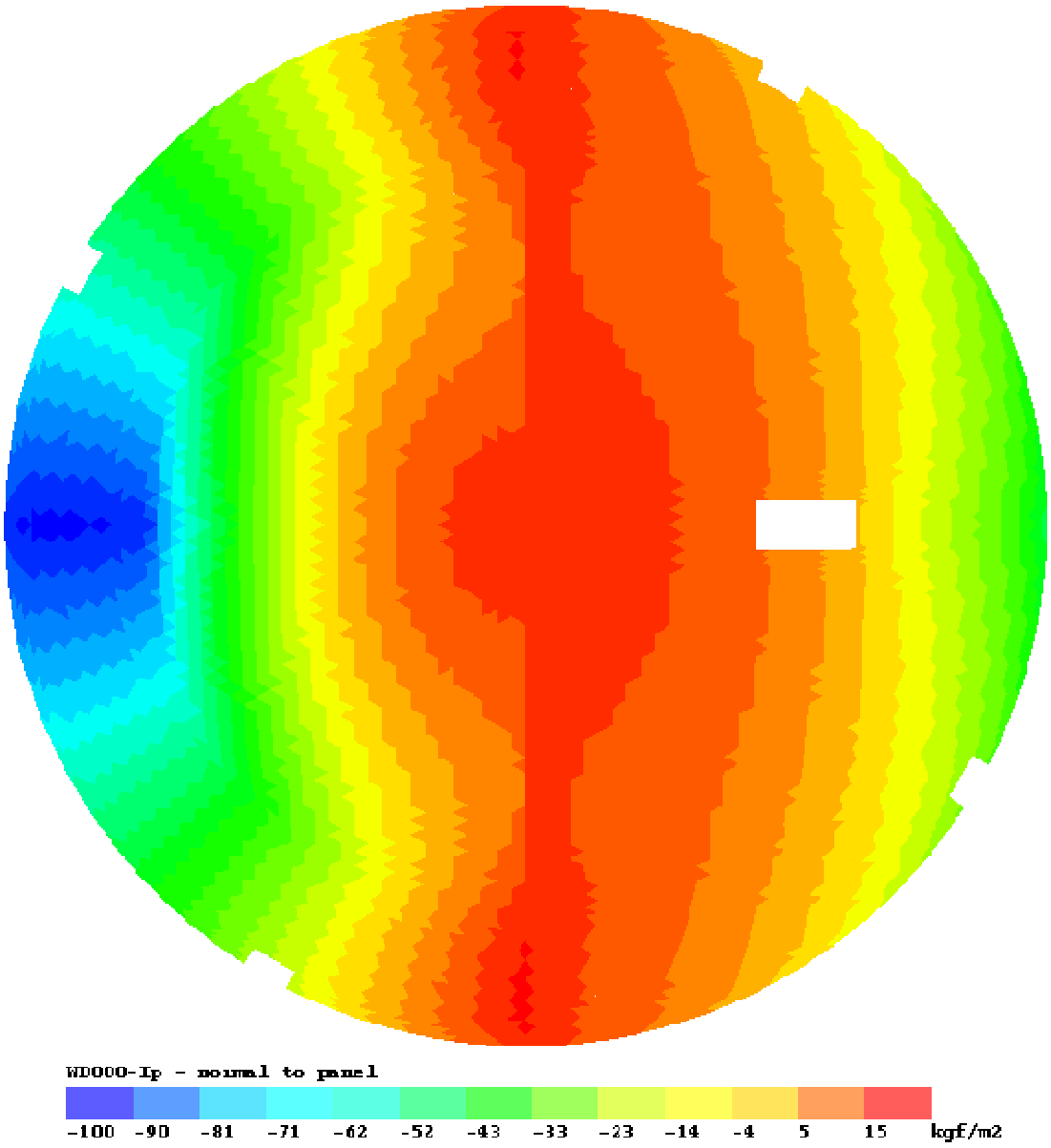

Figure 4.6 Contour for dome with small opening with wind load and internal pressure.

5. RESULTS

5.1 Introduction

This chapter mainly is mainly focused on the result's that are obtained from the simulation cases. It is not possible to show the entire result text file since the data is very large and hence some part of data has been presented here. The results mainly consist of the graphs plotted for different simulation cases and the mode shapes generated by the PATRAN. These results are discussed in detail in the next chapter.

5.2 Results

As mentioned previously the dome with large opening, small opening and small opening with reinforcement were analyzed for buckling under wind load. Wind from different directions has been applied starting with 0 degrees and incrementing 45 degrees. The maximum load factor at which the dome fails obtained for different angles is shown in the table below.

Table 5.1- Load factor for dome with small opening with positive internal pressure

Case / Angle	0	45	90	135	180	225	270	315
Small Opening + Internal Pressure	21.87	17.50	16.38	12.09	20.24	18.00	15.68	20.00

The results obtained clearly shows a large variation in the behavior of the dome with small opening when the wind load is acting from different directions. The dome can carry much higher loads when the wind acts from 0 degrees and least at 135 degrees.

The load factors obtained above were calculated as follows:

The '.dat' file which is generated as MATLAB output has a load factor (LF). This factor is multiplied by the percentage load obtained from the PATRAN results. For example in case of 315 degree wind load for large opening the maximum percentage load at which the dome fail is 111.042 %. In this case the factor (LF) used was 30. The factor for this load is obtained is as follows.

Factor = (111.042 -100) / 100 *30 = 3.31.

The x- axis is the factored load. The y- axis is Normalized Displacement which is a dimensionless quantity. This is obtained by adding the maximum displacement due to wind load and dead load and then divided by the maximum displacement with dead load. All the graphs shown are for one node which fails at maximum load.

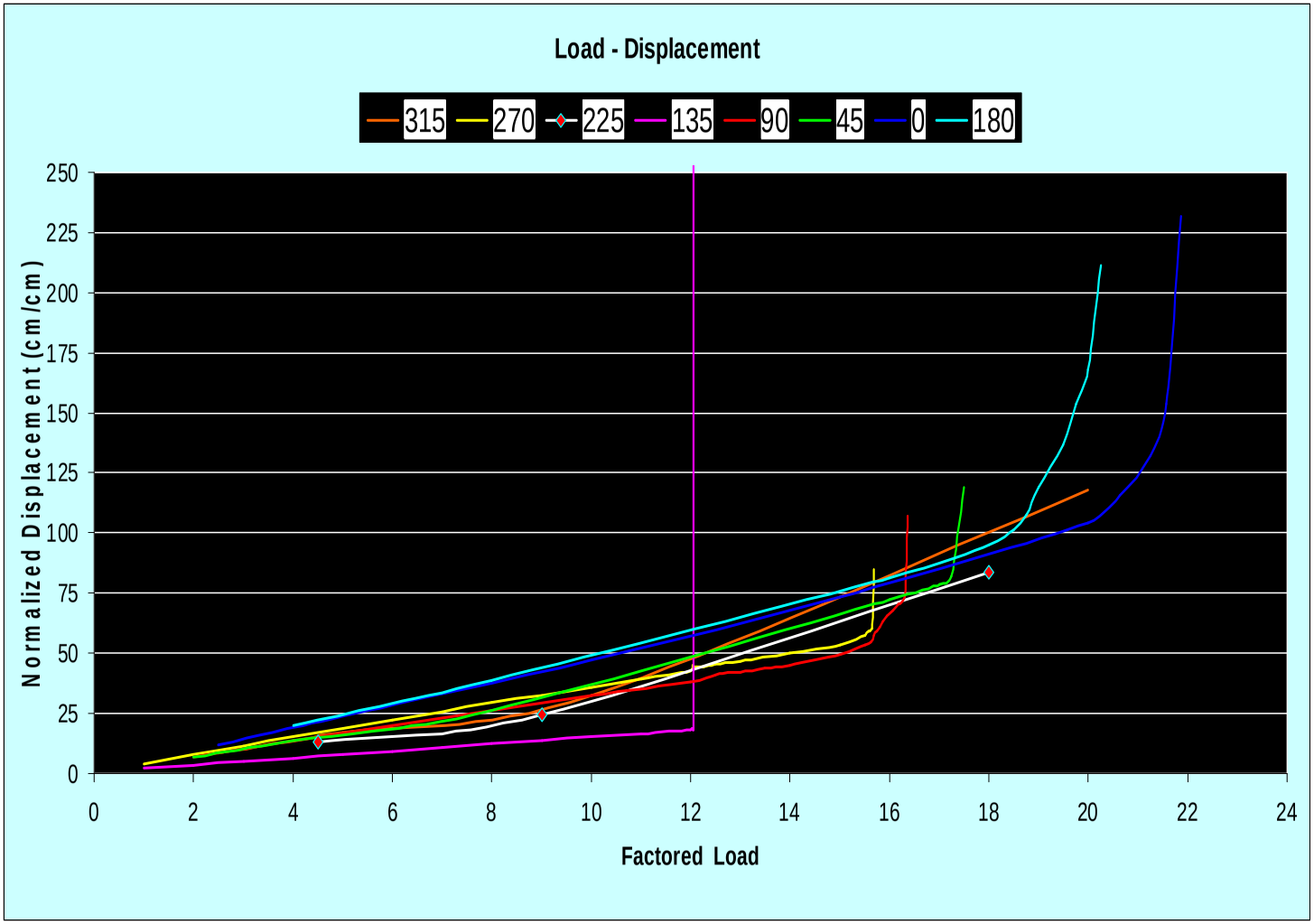

Figure 5.1 Graph comparing wind load acting from different directions (Small Opening, Positive Internal Pressure)

In some of the plots it is seen that the dome carries load even after failing. This is because of the case called snap through buckling where the dome snaps from one stable region to other that is the dome snaps from tension to compression. Therefore the factored mentioned in the above table are at a point where the dome snaps first.

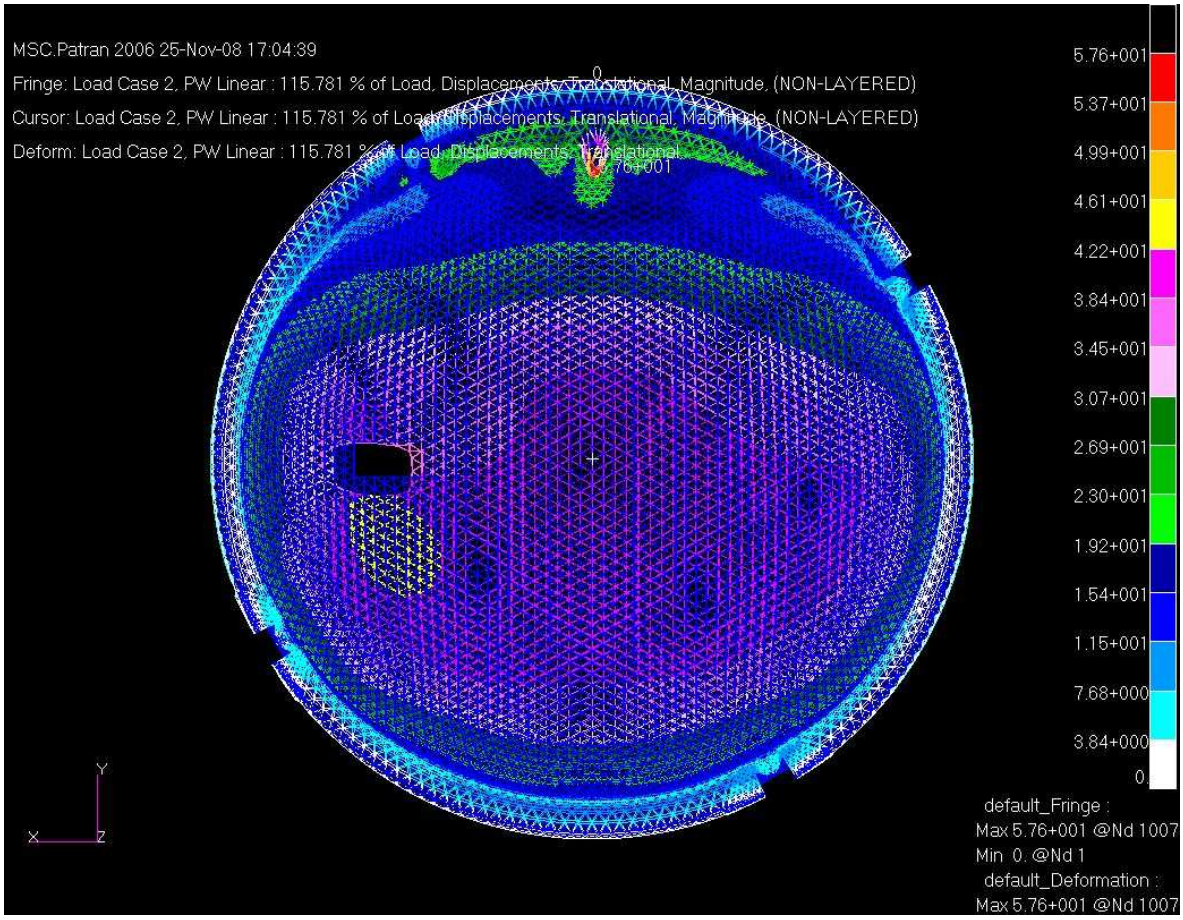

Figure 5.2 Mode shape for dome with small opening and wind acting at 270 degrees.

Table 5.2- Load factor for dome with small opening with reinforcement with positive internal pressure.

Case / Angle	0	45	90	135	180	225	270	315
Reinforcement + Internal Pressure	18.00	12.09	16.37	20.81	15.40	21.37	15.81	12.03

From the above results it can be seen that the dome can carry much greater load when wind acts at angle 225 degrees and least when acting from 45 degrees and 315 degrees. It can also be seen that the factors except for wind acting from 0 degrees and 180 degrees are much similar. For wind acting from 45 degrees and 315 degrees it is around 12, for 135 and 225 it is close with very small difference and same for 90 degrees and 270 degrees.

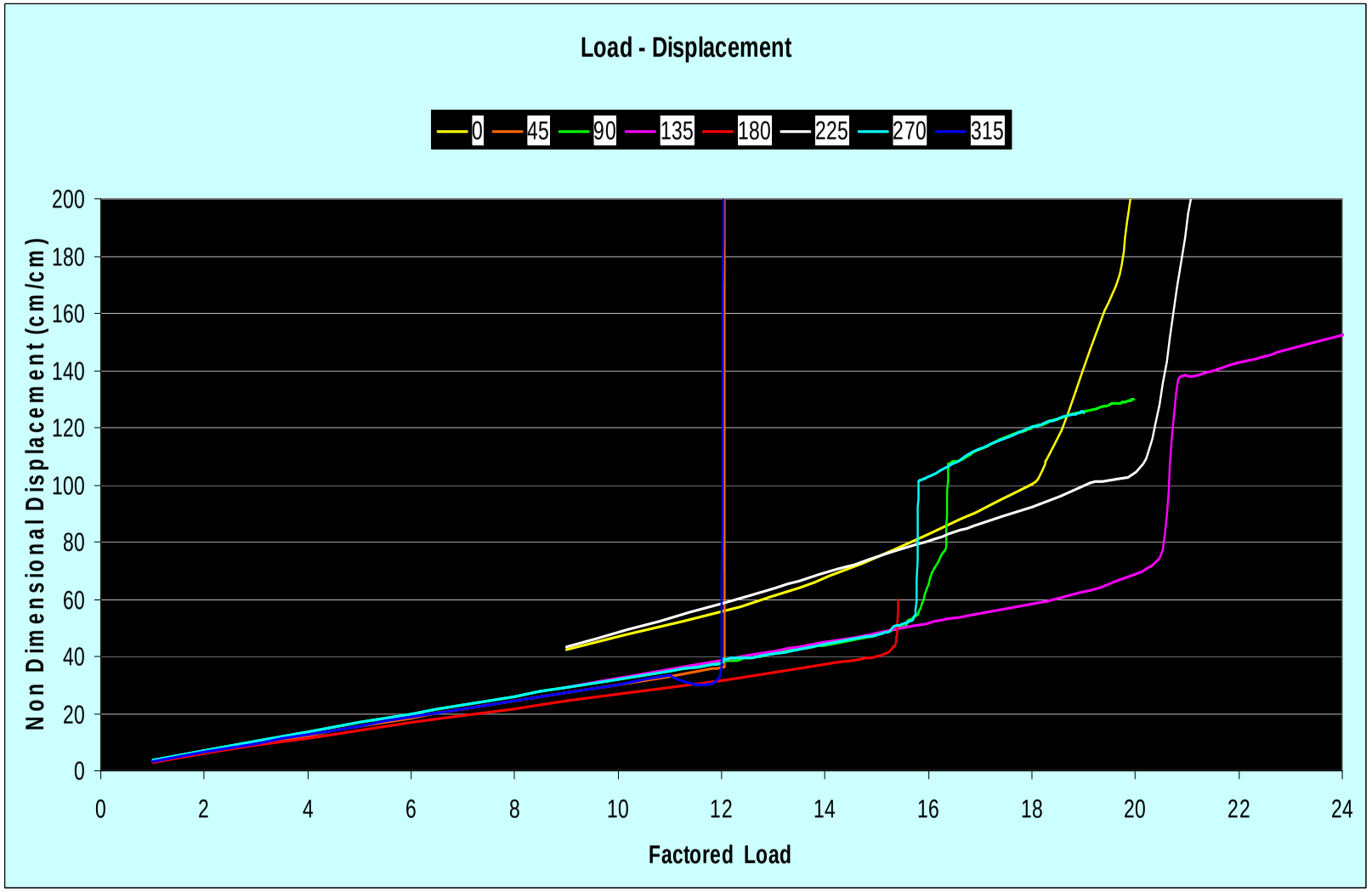

Figure 5.3 Graph comparing wind load acting from different directions (Small Opening with Reinforcement, Positive Internal Pressure)

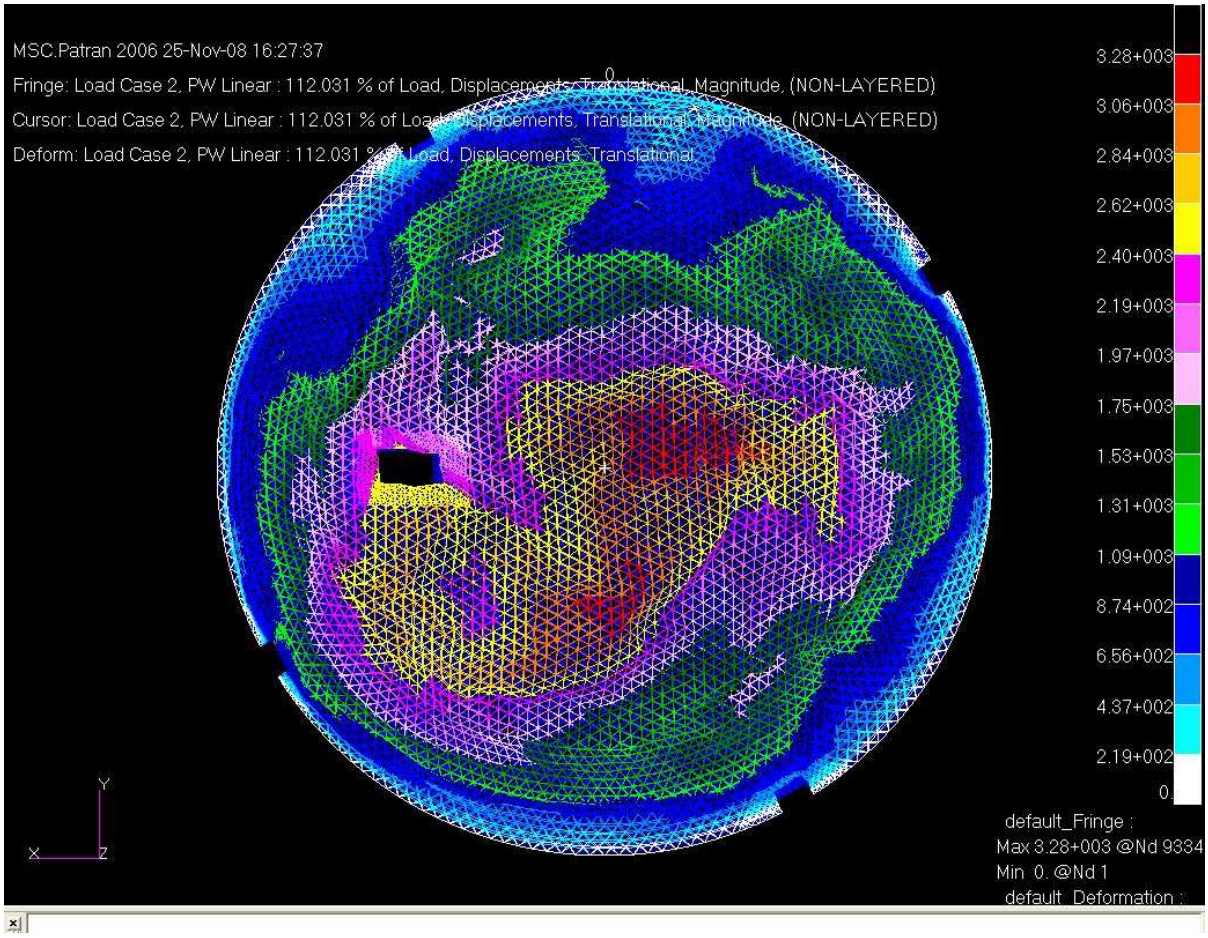

Figure 5.4 Mode shape for dome with small opening with reinforcement with positive internal pressure and wind acting at 315 degrees.

Table 5.3 – Load factor for dome with large opening with positive internal pressure

Case / Angle	0	45	90	135	180	225	270	315
Large Opening + Internal Pressure	-	17.43	19.38	16.06	21.56	19.68	18.00	-

The results obtained clearly show that the dome has higher capacity when the wind load acts from 0 degrees since it is still in tension even after applying a factor of 63. The least factor is 16.06 when wind acts from 135 degrees direction.

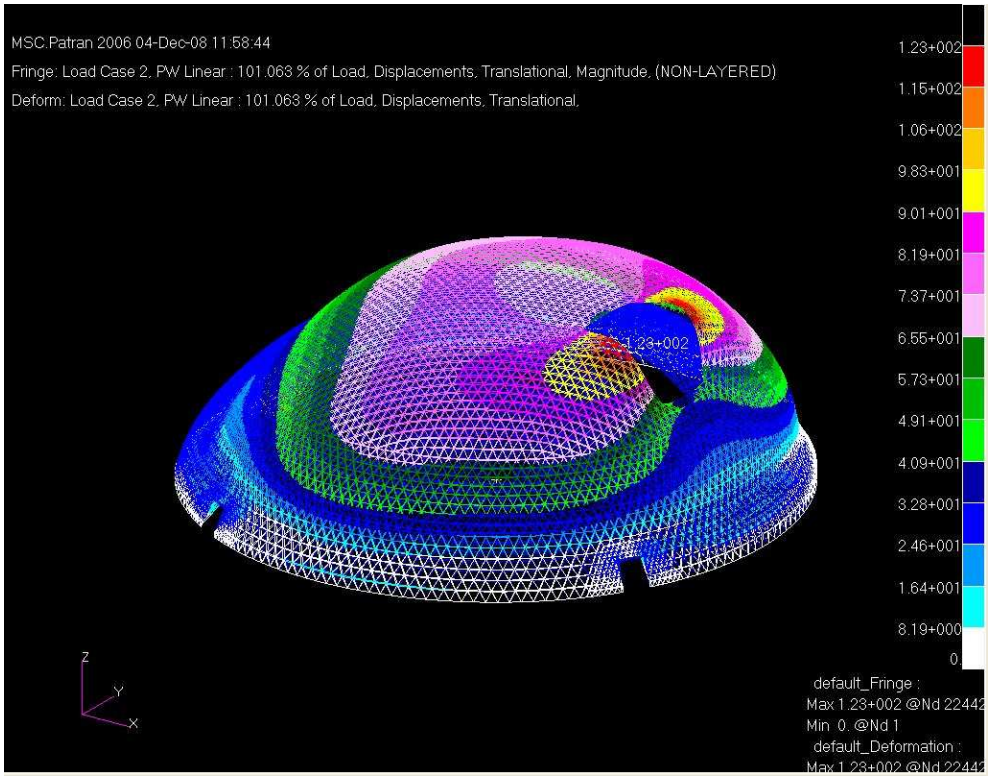

Figure 5.5 Mode shape for dome with large opening with positive internal pressure and wind acting at 0 degrees.

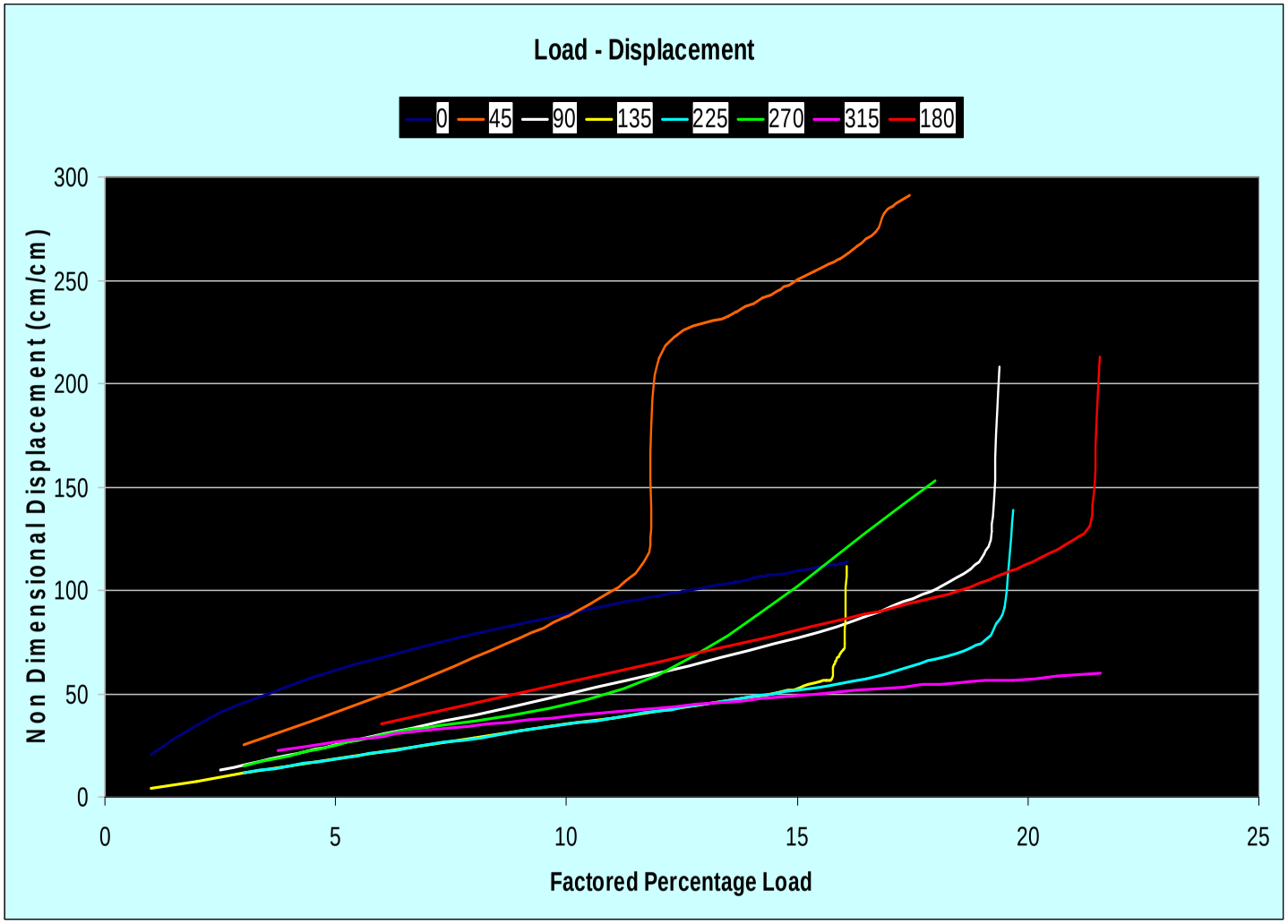

Figure 5.6 Graph comparing wind load acting from different directions (Large Opening, Positive Internal Pressure)

Table 5.4 – Load factor for dome with small opening with negative internal pressure

Case / Angle	0	45	90	135	180	225	270	315
Small Opening - Internal Pressure	3.68	3.36	3.375	3.03	2.87	3.18	3.43	3.24

The load factors obtained from the simulations for the small opening with negative internal pressure show that the dome has less bearing capacity when the dome is in compression. The highest being 3.68 for wind load acting from 0 degrees and the lowest 2.87 when wind acts from 180 degrees angle.

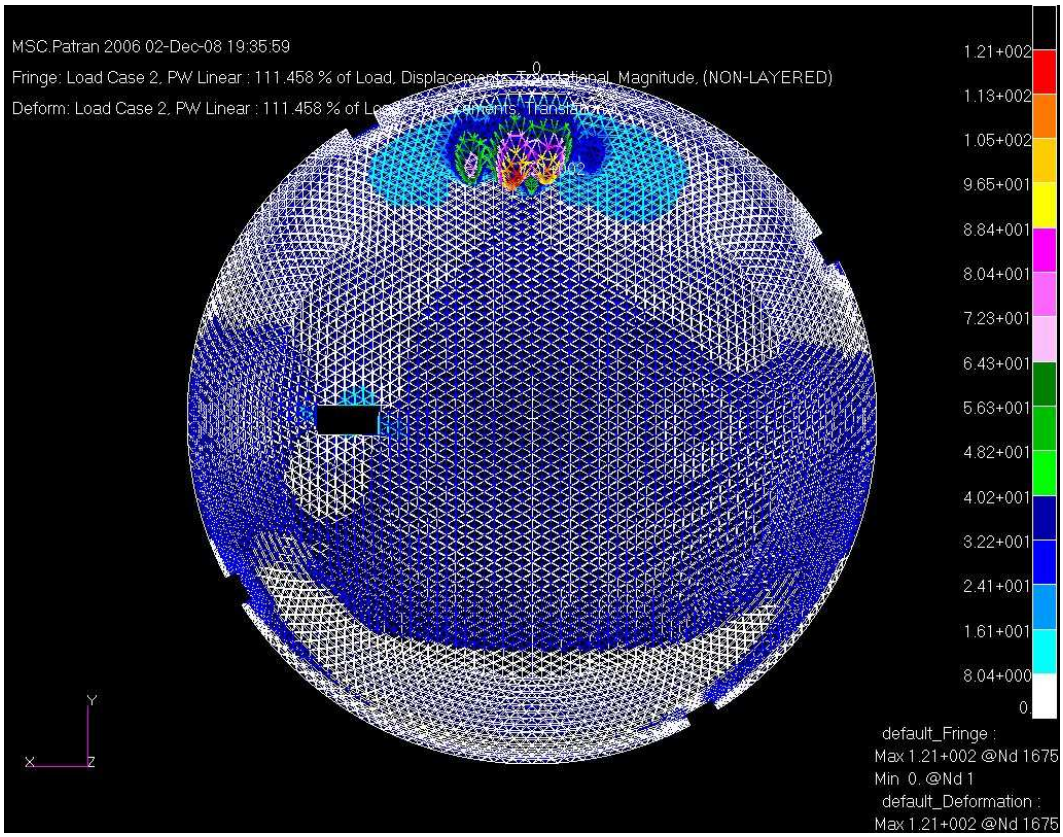

Figure 5.7 Mode shape for dome with small opening with negative internal pressure wind acting at 270 degrees.

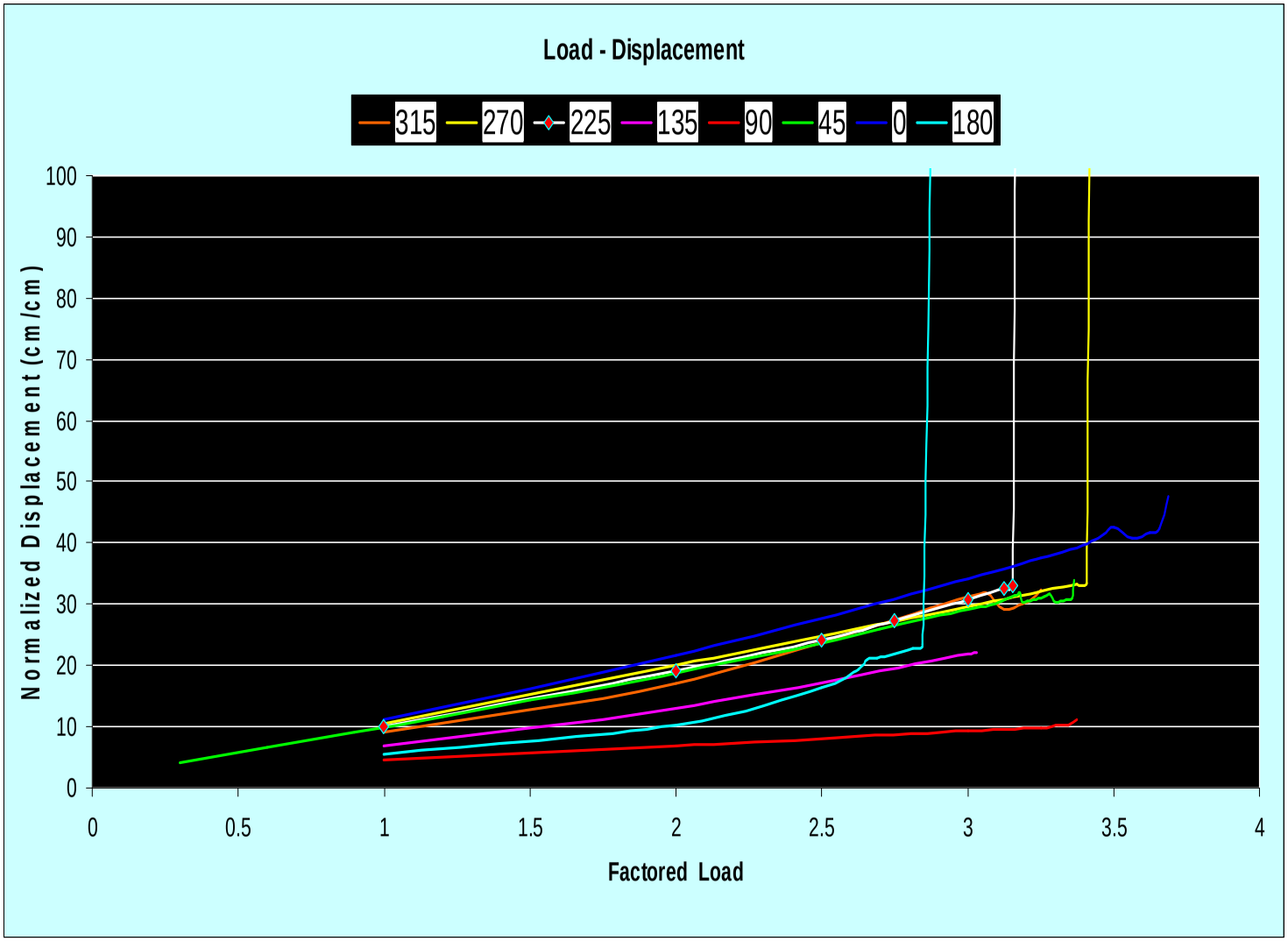

Figure 5.8 Graph comparing wind load acting from different directions (Small Opening, Negative Internal Pressure)

Table 5.5 – Load factor for dome with small opening with reinforcement with negative internal pressure

Case / Angle	0	45	90	135	180	225	270	315
Reinforcement - Internal Pressure	3.30	6.09	3.89	3.18	3.70	3.75	3.89	3.18

The results obtained for dome with small opening with reinforcement show that the dome can carry maximum load when wind load acts from 45 degrees and the least in 135 degrees.

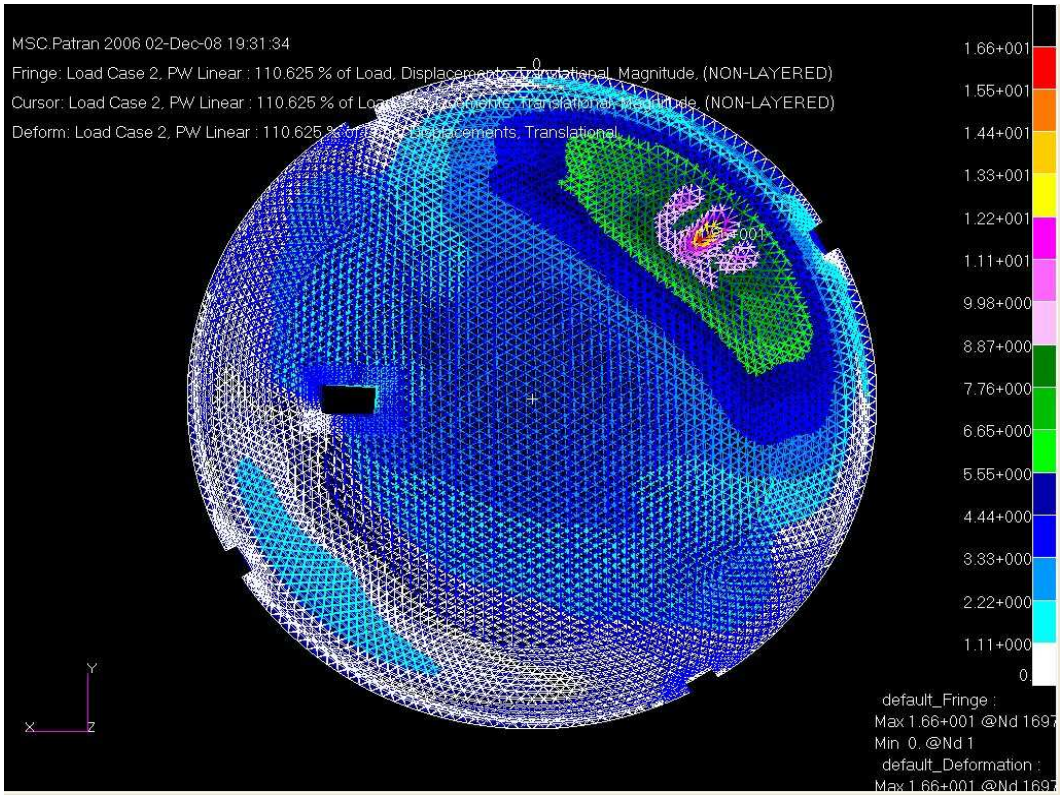

Figure 5.9 Mode shape for dome with small opening with reinforcement with negative internal pressure wind acting at 315 degrees.

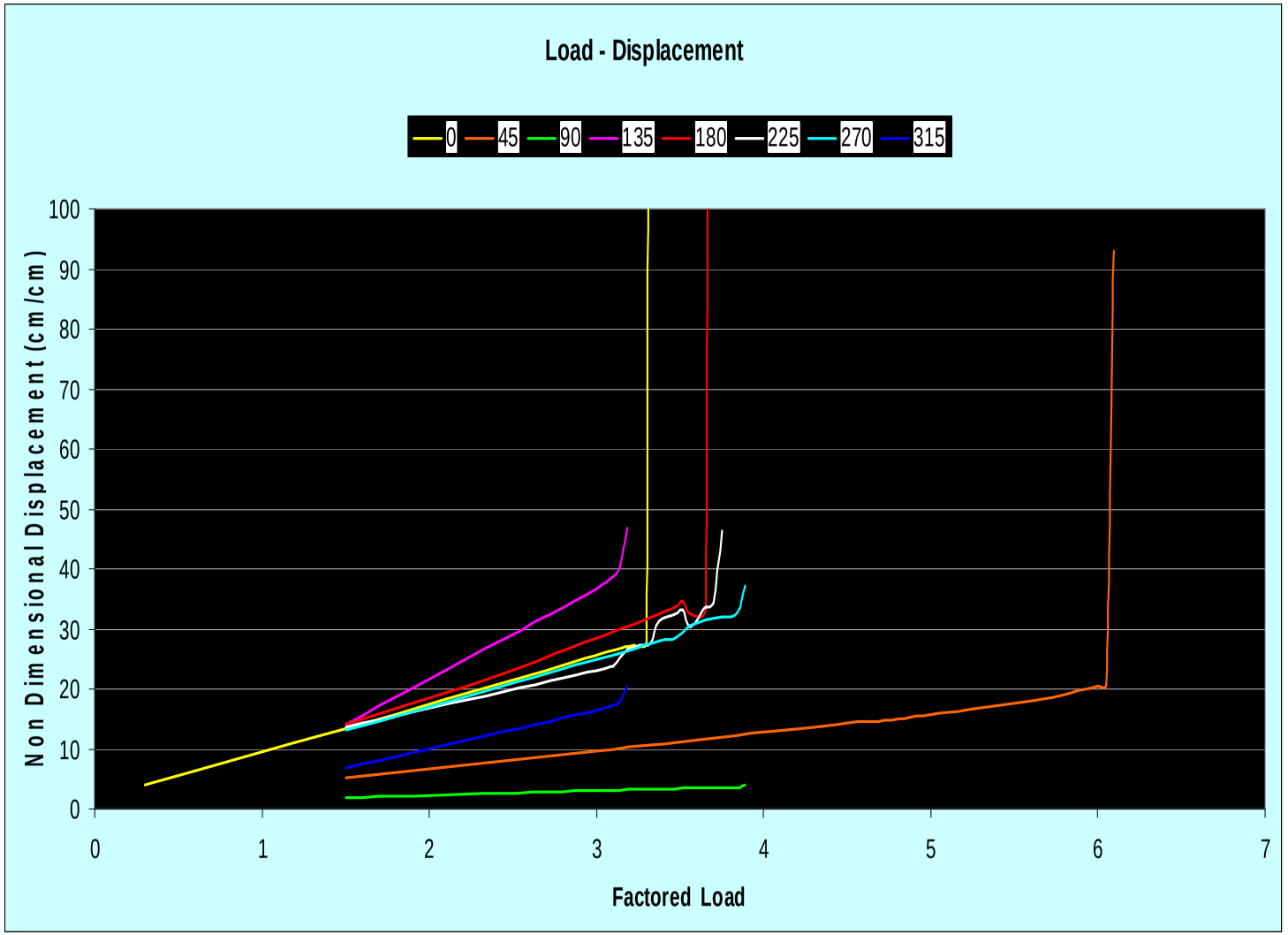

Figure 5.10 Graph comparing wind load acting from different directions (Small Opening with reinforcement, Negative Internal Pressure)

Table 5.6 – Load factor for dome with large opening with negative internal pressure

Case / Angles	0	45	90	135	180	225	270	315
Large Opening - Internal Pressure	3.65	1.56	3.28	2.84	2.49	2.72	3.38	3.31

The load factor in case for the dome with large opening with negative internal pressure is least when wind load acts from 45 degrees and maximum for wind load acting form 0 degrees.

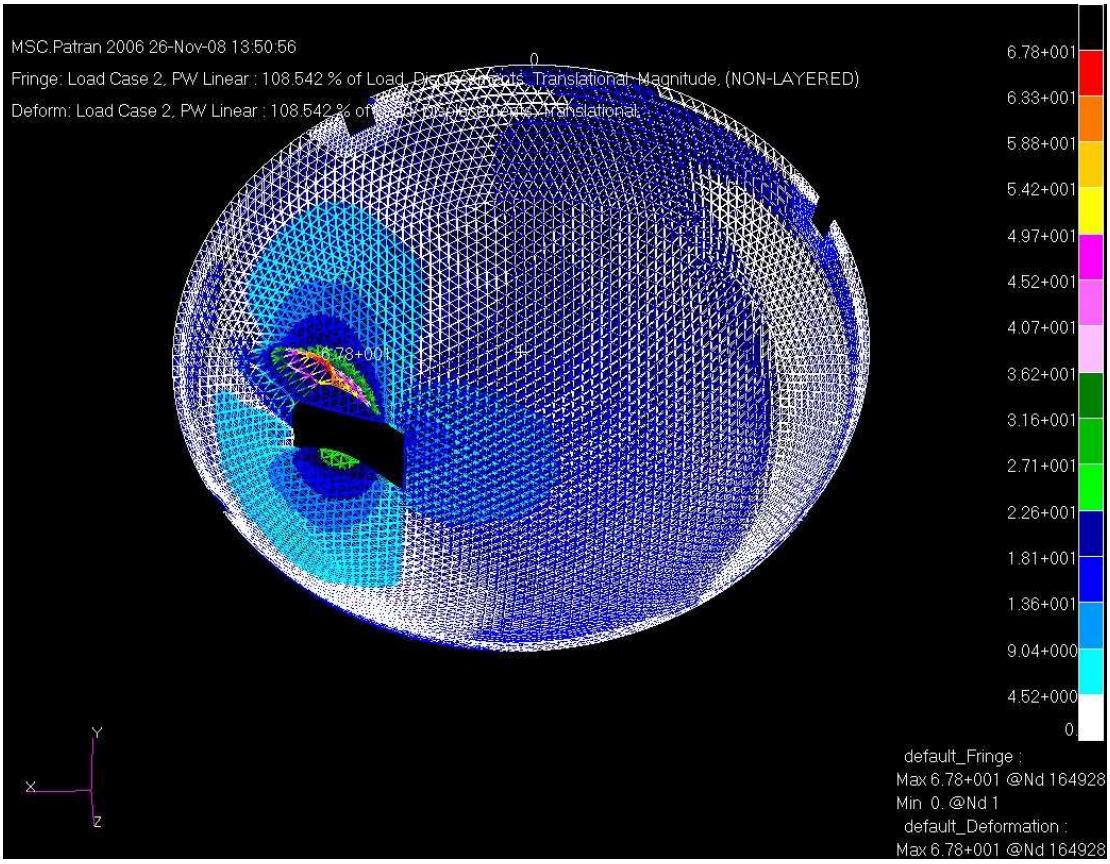

Figure 5.11 Mode shape for dome with large opening with negative internal pressure wind acting at 180 degrees.

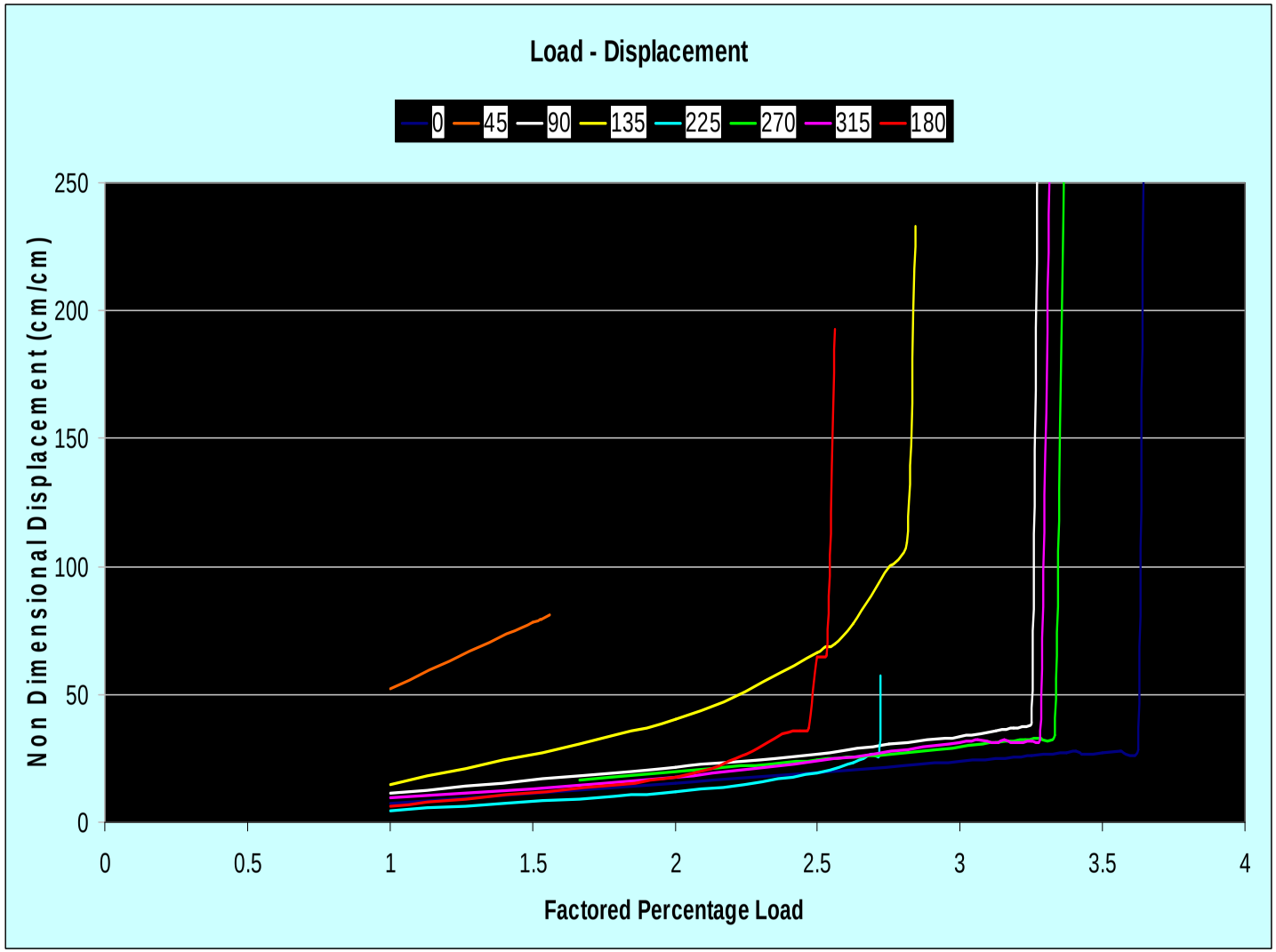

Figure 5.12 Graph comparing wind load acting from different directions (Large Opening, Negative Internal Pressure)

6. SUMMARY AND CONCLUSION

6.1 Summary

Dome structures with different size of openings were analyzed for buckling under wind load acting from different directions. Non linear analysis has been carried out where wind load is incremented till the dome fails. NASTRAN and PATRAN software was used for the analysis. The data for these structures was provided by company 'GEOMETRICA'. A MATLAB program was developed to convert this data to a .dat file which could be read by NASTRAN. The results were viewed in PATRAN.

The size and shape of the dome in all the three case is same except for the size of opening. The first dome had a small opening with size 9.72 m x 4.74 m. The second dome had a large opening with size 16.45 m x 10.74 m. The third dome had same opening size of 9.72 m x 4.74 m one but it was additionally reinforced near the opening. In all the three cases the dome carries its self weight, internal wind pressure and external wind load. The wind load was applied from different directions incrementing every 45 degrees starting from 0 degree angle. The result obtained from this analysis was plotted and were compared for wind load from all directions.

6.2 Conclusion

The results obtained from the simulations for wind load with positive internal pressure show that there is a large variation in the load carrying capacity of the dome. It clearly shows that the position of the opening has major effect on buckling of the dome structure and it cannot

be concluded that placing the dome in any direction will make same effect on the load carrying capacity. It is also seen that the dome can carry much higher load when the wind is acting at an angle 0 degrees that is the opening of the dome directly faces the wind load.

It is also observed that the factor obtained for wind load acting from 315 degrees is more than 45 degrees, 90 degrees is more than 270 degrees, and 225 degrees is more than 135 degrees, which might be possible because of the position of the opening in the roof is not symmetrical to the opening which are used for the walkways.

The factors obtained for the dome with small opening with reinforcement show that reinforcing the opening has no effect on bucking of the dome.

It can also be seen that the factors obtained for positive internal pressure is high than the one obtained for negative pressure. Following are figures showing dome with different opening sizes with negative internal pressure and load factors that control the design.

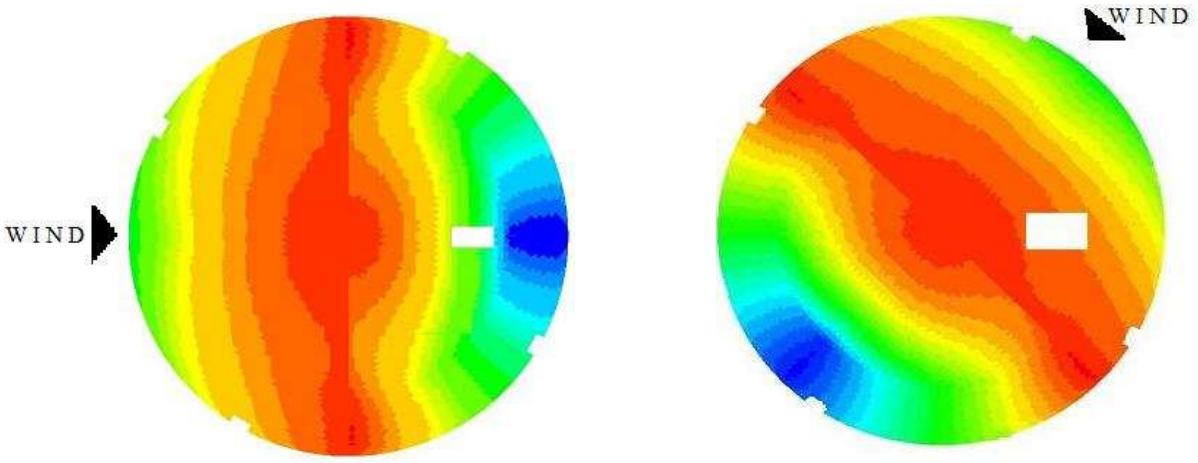

Figure 6.1 **(a)** **(b)**

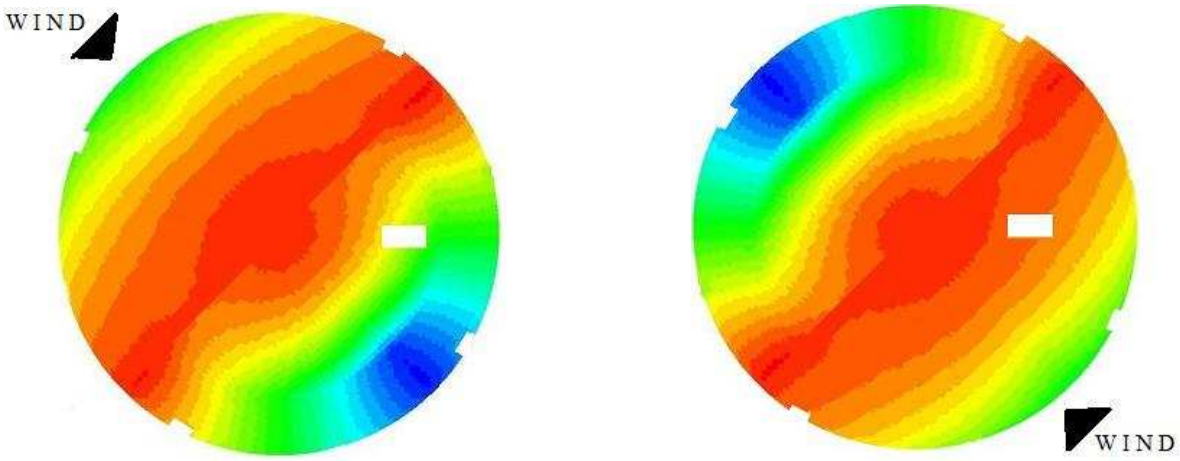

(c) **(d)**

Figure 6.1 (a) Dome with small opening, least load carrying capacity with load factor 2.87 when wind load acts from 180 degrees angle.

(b) Dome with large opening, least load carrying capacity with load factor 1.56 when wind load acts from 45 degrees angle.

(c) Dome with small opening with reinforcement, least load carrying capacity with load factor 3.18 when wind loads acts from 135 degrees angle.

(d) Dome with small opening with reinforcement, least load carrying capacity with load factor 3.18 when wind loads acts from 315 degrees angle.

Since load factors for negative internal pressure are less than the positive internal pressure it can be concluded that, the domes have to be designed for negative internal pressure.

The factors obtained for the dome with small opening with reinforcement show that, reinforcing the opening has no major effect towards improving resistance against bucking of the dome.

6.3 Recommendations

The results presented in this thesis were for the wind loads developed from the ASCE equations. Further studies could be done using wind tunnel test data and comparisons of the critical load could be conducted. In future studies, the location of the opening can also be changed and can be checked for critical load. Based on the results of this study, the members and connections can be redesigned to improve the dome load carrying capacity.

REFERENCES

Wu C. C and Arora. J.S. (1988). “Design Sensitivity Analysis of Nonlinear Buckling Load.”

Kato. S, Mutoh. I, and Shomura. M. (1994). “Effect of Joint Rigidity on Buckling Strength of Single Layer Lattice Domes.”

Fujito.M, Imai. K, and Saka. T. (1994). “Buckling of Single Layer Lattice Domes Under Uniform Gravity Load.”

Ragavan. V. and Made. M.A. (1999). “Nonlinear Buckling and Post Buckling of Cable Stiffened Prestressed Domes.”

Hiyama. Y, Takashima. H, Iijama. T, and Kato. S.(2000). “Buckling Behavior of Aluminium Ball Jointed Single Layer Reticular Domes.”

Ragavan. V, Amde. M. A. (2000). “Nonlinear Stability of Ring Stiffened Prestressed Dome.”

Ragavan. V, Amde. M. A. (2002). “Effect of Stiffeners on Nonlinear Stability of Self Erecting Dome.”

Lopez. A, Puente. I, and Serna. M.A. “Analysis of Single Layer Lattice Domes-A New Beam Element.”

Don O. Blush, Bo O. Almroth. “Buckling of Bars, Plates, and Shells.” (1975) “Mc Graw-Hill Inc.”

Zdenek P. Bazant, Luigi Cedolin. “Stability of Structures.” (1991) “Oxford University Press.”

MSC NASTRAN 2005 Documentation.

www.efunda.com, Elastic Buckling of Columns.

APPENDIX

Data file for dome with small opening and wind load acting for 135 degrees with positive internal pressure

```
$Run with mem=90mw
ASSIGN OUTPUT2='Star_Cement_WeakOpNew_NonLinearINC.op2',UNIT=12
ID GEOMETRICA
SOL 106
CEND
TITLE=Star_Cement_WeakOpNew_NonLinearINC
ECHO=NONE
MAXLINES = 999999999
$STRESS=ALL
SET 80=846012
  OLOAD=80
SPC=12
DISP=ALL
SUBCASE 1
  NLPARM=10
  LOAD=10000
SUBCASE 2
  NLPARM=20
  LOAD=20000
BEGIN BULK
$ GEOMETRY
GRID,1,,    0.00, 5207.50,    52.9
GRID,2,, -194.71, 5203.86,    52.9
GRID,3,, -389.16, 5192.94,    52.9
.
.
.
$ CONNECTIVITY
CBEAM,2,2,2,3, -0.0561,  0.9984, -0.0000
 + 0, 0
CBEAM,3,3,3,4, -0.0934,  0.9956, -0.0000
 + 0, 0
CBEAM,4,4,4,5, -0.1305,  0.9914, -0.0000
.
.
.
```

```
$ PROPERTIES
PBEAM,2,1,    3.26,   13.80,    0.06,,   13.85
+,    7.13,    0.00,   -7.13,    0.00,    0.00,    0.23,    0.00,   -0.23
+,NO  , 0.0466,    3.26,    8.39,    8.39,,   16.78
+,NO  , 0.9534,    3.26,    8.39,    8.39,,   16.78
+,YESA, 1.00,    3.26,   13.80,    0.06,,   13.85
+,0.0,0.0
PBEAM,3,1,    3.26,   13.80,    0.06,,   13.85
+,    7.13,    0.00,   -7.13,    0.00,    0.00,    0.23,    0.00,   -0.23
+,NO  , 0.0466,    3.26,    8.39,    8.39,,   16.78
+,NO  , 0.9534,    3.26,    8.39,    8.39,,   16.78
+,YESA, 1.00,    3.26,   13.80,    0.06,,   13.85
+,0.0,0.0
.
.
.
MAT1,1,2038891.4,,0.30,0.000000,0.000023,    0.00
$MATS1,1,,PLASTIC,0.,,,  2952.9
.
.
.
$ LOADING
FORCE,100,1,,1.0,    0.00,    0.00,  -33.17
FORCE,100,2,,1.0,    0.00,    0.00,  -33.17
FORCE,100,3,,1.0,    0.00,    0.00,  -33.17
FORCE,100,4,,1.0,    0.00,    0.00,  -33.17
.
.
.
LOAD,10000,1.0,  1.0000,100 (Dead Load Factor)
LOAD,20000,100.0,  1.0000,300,  1.0000,700 (Wind Load Factor)
$ CONSTRAINTS
SPC,12,1,123
SPC,12,2,123
SPC,12,3,123
.
.
.
$ PARAMETERS
PARAM,POST,-1
PARAM,LGDISP,2
NLPARM, 10,  5, , AUTO, , , , YES
NLPARM, 20, 100, , AUTO,1, , , YES
ENDDATA
```

CURRICULUM VITAE

Anup Ramesh Marathe was born on April 8, 1982 in Maharashtra, India. He completed his schooling from St Patrick's High School , Secunderabad in 1997 and Higher Secondary School in 1999 from J.V.S College, Hyderabad. He graduated from Marathwada Institute of Technology, Aurangabad, India in Spring 2004.

After completing his Bachelor's Degree in Civil Engineering he worked as Design Engineer for 28 months and then got admit to The University of Texas at El Paso in Spring 2007 for Masters program in Civil Engineering majoring towards structures. While pursuing his Masters degree he worked as Graduate Teaching Assistant from Spring 2007 to Spring 2009. He also worked as a Research Assistant at the same time for a project which was offered by company 'GEOMETRICA'.

Permanent Address:

H.No 8-7-63/1C, Road No 10. North

R.R Nagar, Old Bowenpally

Secunderabad-500011

India.